

# Stability and robustness of large platoons of vehicles with double-integrator models and nearest neighbor interaction

He Hao\*, Prabir Barooah

## SUMMARY

We study the stability and robustness of a large platoon of vehicles, where each vehicle is modeled as a double integrator, for two decentralized control architectures: predecessor-following and symmetric bidirectional. In the predecessor-following architecture, the control action on each agent only depends on the information from its immediate front neighbor, while in the symmetric bidirectional architecture, it depends equally on the information from both its immediate front neighbor and back neighbor. We prove asymptotic stability of the formation for a class of nonlinear controllers with sector nonlinearity, with the linear controller as a special case. We show the convergence rate of the predecessor-following architecture is much faster than that of the symmetric bidirectional architecture. However, the predecessor-following architecture suffers high algebraic growth of initial errors. We also establish scaling laws (with  $N$ ) of certain  $H_\infty$  norms of the formation that measure its robustness to external disturbances for the linear case. It is shown that the robustness performance grows geometrically in  $N$  for predecessor-following architecture, but only polynomially in  $N$  for symmetric-bidirectional architecture. Extensive numerical simulations are conducted to verify the predictions for the linear case and empirically estimate the corresponding performance metrics for a saturation-type nonlinear controller. Based on the analytical and numerical results, it is seen that the symmetric bidirectional architecture outperforms the predecessor-following architecture in all measures of performance. Within the predecessor-following architecture, the non-linear controller is seen to perform better in general than the linear one. A number of design guidelines are provided based on these conclusions. Copyright © 2012 John Wiley & Sons, Ltd.

Received . . .

KEY WORDS: Multi-agent systems; Convergence rate;  $H_\infty$  norm; Nonlinear control; Distributed control

## 1. INTRODUCTION

Cooperative control of multi-agent systems has spurred an extensive interest in the control community because of its wide range of applications such as automated highway system [1, 2], coordination of aerial, ground, and autonomous vehicles for surveillance and rescue [3], spacecraft formation control for science missions [4], and collective behavior of bird flocks and animal swarms [5]. Among these applications, one of the most well studied problems is autonomous intelligent cruise control of large vehicular platoons, see [6, 7, 8, 9] and the reference therein. The primary goal of autonomous intelligent cruise control is to increase traffic throughput and safety.

One of the most important problems in autonomous intelligent cruise control of platoons is string instability or slinky-type effect [10, 11, 12]. To solve this problem, different control policies and control architectures are considered. In [11], a constant headway control law is developed to insure string stability. However, the constant headway policy by itself is not enough, the headway has

---

\*Correspondence to: He Hao. He Hao and Prabir Barooah are with Department of Mechanical and Aerospace Engineering, University of Florida, Gainesville, FL 32611, USA. Email: hehao, pbarooah@ufl.edu. This work was supported by the National Science Foundation through Grants CNS-0931885 and ECCS-0925534.

to be *large enough* to avoid the problems associated with constant spacing policy [13]. Since one of the main motivations for automated platooning is to achieve higher highway capacity by making cars move with a small inter-vehicle separation, there is a need to study the constant spacing policy. It was shown in [11, 14, 15] that with constant spacing policy, the leader's information need to be broadcasted to the following vehicles to assure string stability. Nevertheless, the inevitable time delay and package drop in broadcasting the leader's information will cause string instability [16]. This leads to the study of decentralized control architecture, i.e. each vehicle can only use measurements of relative position and/or velocity with respect to its nearest neighbors.

Two decentralized control architectures that are commonly examined are predecessor-following and bidirectional architectures. In the *predecessor-following* architecture, the control action on each vehicle only depends on the relative information from its immediate predecessor, i.e. the vehicle in front of it. In the bidirectional architecture, the control depends on the relative information from both its immediate predecessor and follower. Within the bidirectional architecture, the most commonly analyzed case is the *symmetric bidirectional* architecture, in which the control at a vehicle depends on the information from both of its neighbors *equally*.

A typical issue in distributed/decentralized control is that as the number of agents in the system increases, the performance of the closed-loop degrades progressively. It has been established that the predecessor-following architecture suffers from high sensitivity to external disturbances with linear control [17, 18]. High sensitivity to external disturbance is typically referred to as slinky-type effect [19, 20] or string instability [21]. Seiler *et al.* showed that with linear control, the poor robustness performance with the predecessor-following architecture is independent of the design of the controller, but a fundamental artifact of the architecture [14]. The robustness performance can be improved by non-identical linear controllers but at the expense of the control gains increasing without bound as the number of the vehicles increases [11, 22]. It was shown in [14, 23, 15, 21] that the symmetric bidirectional architecture also suffers from poor sensitivity to external disturbances.

Although a rich literature exist on sensitivity to disturbances for predecessor-following and symmetric bidirectional architectures with linear control, to the best of our knowledge, a precise comparison of these two architectures is lacking. Moreover, most of the works on formation control have been limited to linear control laws, while little is known about nonlinear control. Nonlinear terms in the closed loop dynamics may arise from either purposefully designed nonlinear control laws (if beneficial) or unavoidable non-linearities in the agent dynamics, such as actuator saturation. Both of these cases can be analyzed by considering linear plant dynamics and nonlinear controllers.

In this paper we examine the stability and robustness (sensitivity to external disturbances) of large platoon of vehicles with linear as well as a class of nonlinear controllers, for both predecessor-following and symmetric bidirectional architectures. Each vehicle is modeled as a fully actuated point mass (double-integrator). A few authors have used first order kinematic models by ignoring vehicle inertia. However, in general kinematic models (single integrator) fail to reproduce the slinky-type effects that are exhibited by kinetic models (double integrator).

We prove stability of the closed loop with an arbitrary number of agents for a class of non-linear controllers where the control gain functions satisfy certain sector conditions. The difference between the transient responses of the two architectures in case of linear control is explained by the expressions we derive for the least stable eigenvalue of the closed-loop state matrix and its multiplicity. In particular, we show that the predecessor-following architecture has a larger convergence rate compared to the symmetric bidirectional architecture:  $O(1)$  vs.  $O(1/N^2)$ . It is worthwhile to mention the convergence rate of the formation with symmetric bidirectional architecture scales poorly as a function of  $N$  even with centralized LQR control [24]. The real part of the least stable eigenvalue with LQR control scales as  $O(1/N)$ . However, the predecessor-following architecture suffers from algebraic growth of initial conditions due to the high multiplicity of the least stable eigenvalue. For the non-linear control, we study the transient performance through numerical simulations. The simulations show that in the predecessor-following architecture, the transient response is significantly improved by using a saturation-type non-linearity in the control gain instead of a linear control.

Next, we examine the closed-loop's performance in terms of the sensitivity to external disturbances. Specifically, we examine the *first-to-last amplification factor*, defined as the  $L_2$  gain from a disturbance injected at the first vehicle to the position tracking error of the last vehicle and *all-to-all amplification factor*, which is defined as the  $L_2$  gain from the disturbances acting on all the vehicles to their position tracking errors. In case of linear controllers, we show that when  $N$  is large, the first-to-last amplification factor, which becomes a  $H_\infty$  norm, grows as  $O(\alpha^N)$ ,  $\alpha > 1$ , for predecessor-following architecture but only as  $O(N)$  for the symmetric bidirectional architecture. The all-to-all amplification factor scales as  $O(\alpha^N)$  for predecessor-following architecture while as  $O(N^3)$  for the symmetric bidirectional architecture. The first result is known in the literature [14]. These results establish a precise comparison between the robustness of symmetric bidirectional and predecessor-following architectures with linear control. Namely, symmetric bidirectional architecture has a much smaller sensitivity to external disturbances.

Establishing scaling laws for robustness metrics with non-linear controllers is challenging. We therefore study the response in the non-linear case through extensive numerical simulations, with both sinusoidal and random disturbances as inputs, and estimate performance metrics from simulation data. We observe from these studies that, within the predecessor-following architecture, a nonlinear controller with a saturation-type non-linearity performs better than the corresponding linear one. In the symmetric bidirectional architecture, the difference between the linear and nonlinear controller's performance is not significant.

The theoretical as well as numerical simulations lead to certain design guidelines. Comparing all four combinations (linear, non-linear, predecessor following and symmetric bidirectional), we observe that for the same number of agents, the symmetric bidirectional architecture performs considerably better (both in terms of transient decay and robustness to disturbances) than the predecessor following one, and this conclusion is valid for both the linear and non-linear control laws. Thus, the added complexity and cost of the symmetric bidirectional architecture due to additional sensors is justified. If stringent cost considerations allow only the predecessor following architecture, then the non-linear controller should be used over the linear one. Even with a linear control law actuator saturation will make the overall system closer to the closed loop non-linear system studied. Therefore, the fact that both the linear and nonlinear controllers with sector nonlinearities are seen to perform comparably in the symmetric bidirectional architecture can be seen as a "robustness to modeling errors" of this architecture. Some of the results for the linear predecessor following case may be known or easily derived from existing results. We nevertheless include them for the sake of completeness.

The conclusions about the architectures are derived only for the specific control laws we investigated. The local control laws at the vehicles are either of PD (proportional-derivative) type (in the linear case), or such that their linearization around the origin are of PD-type (in the non-linear case). Nevertheless, analysis carried out with this controller structure and double integrator vehicle models is relevant even if there are additional dynamic elements in the loop (i.e, either in the controller or in the vehicle dynamic model), at least in the linear case. Reasons for this can be seen from the results in [23], which considered vehicle models with two integrators in series with an additional transfer function (to model powertrain dynamics) and arbitrary LTI compensators. First, a dynamic controller cannot have a zero at the origin since it will result in a pole-zero cancellation causing the steady-state errors to grow without bound as  $N$  increases [23]. Second, a dynamic controller cannot have an integrator either if the vehicle model has two integrators. For if it does, the closed-loop platoon dynamics become unstable for a sufficiently large values of  $N$  [23]. As a result, any allowable dynamic element in the loop must essentially act as a static gain at low frequencies. The results of [23] indicate that the principal challenge in controlling a platoon of vehicles arises due to the presence of a double integrator with its unbounded gain at low frequencies. Hence, the issues discussed here with a PD controller structure is also relevant to the case where additional dynamic elements appear in the loop.

In terms of the stability analysis with non-linear controllers, our work closely parallels that of [25], which considers arbitrary information graphs (instead of the 1-D graph of a platoon we consider). However, the results of [25] are not applicable to the scenario considered here, since we

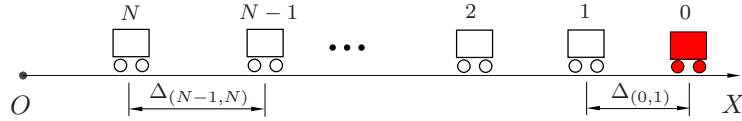


Figure 1. Desired geometry of a 1-D network of  $N$  double-integrator agents. The reference agent with index “0” need not to be real agent, it merely provides the reference trajectory of the formation to agent 1.

consider relative velocity feedback while [25] considers absolute velocity feedback. Furthermore, the assumption of symmetry made in [25] precludes the predecessor-following architecture from their formulation. In terms of sensitivity to external disturbances with linear control, our work is related to [26, 27, 28] and [29, 30]. In [26, 27], it is shown that if the information graph used is undirected and has bounded degree, the maximum error due to sinusoidal disturbances can not be made independent of the size of the formation. In [28], Veerman showed that the first-to-last amplification grows linearly in  $N$  for the symmetric bidirectional case, but grows exponentially in  $N$  for *asymmetric* bidirectional architecture, where asymmetric means the information from its front and back neighbor are weighted differently. Scaling laws of certain  $H_2$  norms from disturbance to outputs that quantify a number of performance measures are examined in [29, 30]. In particular, it was shown that the “all-to-all”  $H_2$  norm scales exponentially in  $N$  for predecessor-following architecture (although with absolute velocity feedback) [30], but as  $O(N^3)$  for the symmetric bidirectional architecture [29], which is the same as that of the all-to-all  $H_\infty$  norm established in this paper. They also show that the scaling laws for the  $H_2$  norm hold for arbitrary but fixed number of front and back neighbors and arbitrary stabilizing feedback gains.

The rest of this paper is organized as follows. Section 2 presents the problem statement. Section 3 and Section 4 present the stability and robustness analysis, respectively, along with corresponding numerical studies. The paper ends with a summary in Section 5.

## 2. PROBLEM STATEMENT

We consider the formation control of  $N$  homogeneous agents which are moving in 1-D Euclidean space, as shown in Figure 1. The position of the  $i$ -th agent is denoted by  $p_i$  and each agent is modeled as a double integrator:

$$\ddot{p}_i = u_i + w_i, \quad i \in \{1, 2, \dots, N\}, \quad (1)$$

where  $u_i$  is the control input, and  $w_i$  is the external disturbance. This is a commonly used model for vehicle dynamics in studying vehicular platoons, and results from feedback linearization of non-linear vehicle dynamics [11, 31].

The control objective is to make the network of agents maintain a rigid formation geometry while following a desired trajectory. The desired geometry of the formation is specified by the *desired gaps*  $\Delta_{(i-1,i)}$  for  $i \in \{1, \dots, N\}$ , where  $\Delta_{(i-1,i)}$  is the desired value of  $p_{i-1}(t) - p_i(t)$ . The desired inter-vehicular gaps  $\Delta_{(i-1,i)}$ 's are positive constants and they have to be specified in a mutually consistent fashion,  $\Delta_{(i,k)} = \Delta_{(i,j)} + \Delta_{(j,k)}$  for every triple  $(i, j, k)$  where  $i \leq j \leq k$ . The desired trajectory of the formation is provided in terms of a *fictitious* reference agent with index 0, whose trajectory is denoted by  $p_0^*(t)$ . The information on the desired trajectory of the formation is only provided to agent 1. The desired trajectory of the  $i$ -th agent,  $p_i^*(t)$ , is given by

$$p_i^*(t) = p_0^*(t) - \Delta_{(0,i)} = p_0^*(t) - \sum_{j=1}^i \Delta_{(j-1,j)}. \quad (2)$$

In this paper, we consider the following two *decentralized* control architectures:

1. *Predecessor-following architecture*. The control action at the  $i$ -th agent depends on the relative position and velocity measurements from its immediate front neighbor. In particular, we

consider the following decentralized control law:

$$u_i = -f(p_i - p_{i-1} + \Delta_{(i-1,i)}) - g(\dot{p}_i - \dot{p}_{i-1}), \quad (3)$$

where  $i \in \{1, 2, \dots, N\}$  and  $f, g : \mathbb{R} \rightarrow \mathbb{R}$  are scalar functions.

2. *Symmetric bidirectional architecture.* The control action at the  $i$ -th agent depends on the relative position and velocity measurements from its immediate front and back neighbors, and the information from its front and back neighbors are weighted equally. In particular, we consider the following decentralized control law:

$$\begin{aligned} u_i &= -f(p_i - p_{i-1} + \Delta_{(i-1,i)}) - g(\dot{p}_i - \dot{p}_{i-1}) \\ &\quad - f(p_i - p_{i+1} - \Delta_{(i,i+1)}) - g(\dot{p}_i - \dot{p}_{i+1}), \\ u_N &= -f(p_N - p_{N-1} + \Delta_{(N-1,N)}) - g(\dot{p}_N - \dot{p}_{N-1}), \end{aligned} \quad (4)$$

where  $i \in \{1, 2, \dots, N-1\}$  and  $f, g : \mathbb{R} \rightarrow \mathbb{R}$ .

In both architectures, the information needed to compute the control action at each agent can be easily obtained by on-board sensors such as radars, since only relative position and velocity are used in the control.

In this paper, we make the following assumptions.

*Assumption 1*

In the above controllers (3) and (4), the possibly nonlinear functions  $f, g : \mathbb{R} \rightarrow \mathbb{R}$  are odd functions, which are smooth enough to guarantee the existence of solution of the coupled ODEs. Each agent  $i$  knows the desired gaps  $\Delta_{(i-1,i)}$ ,  $\Delta_{(i,i+1)}$ , while only agent 1 knows the desired trajectory  $p_0^*(t)$  of the fictitious reference agent. The reference trajectory is a constant velocity type, i.e.,  $p_0^*(t) = v_0 t + c_0$  for some constants  $v_0, c_0$ . The first agent must have access to its own absolute position and velocity information.  $\square$

To facilitate analysis, we define the following position tracking error:

$$\tilde{p}_i := p_i - p_i^*, \quad (5)$$

where  $p_i^*$  is given by (2). The closed-loop dynamics for the predecessor-following architecture can now be expressed as the following coupled-ODE model

$$\ddot{\tilde{p}}_i = -f(\tilde{p}_i - \tilde{p}_{i-1}) - g(\dot{\tilde{p}}_i - \dot{\tilde{p}}_{i-1}) + w_i, \quad i \in \{1, 2, \dots, N\}. \quad (6)$$

The closed-loop dynamics for the symmetric bidirectional architecture are

$$\begin{aligned} \ddot{\tilde{p}}_i &= -f(\tilde{p}_i - \tilde{p}_{i-1}) - g(\dot{\tilde{p}}_i - \dot{\tilde{p}}_{i-1}) - f(\tilde{p}_i - \tilde{p}_{i+1}) - g(\dot{\tilde{p}}_i - \dot{\tilde{p}}_{i+1}) + w_i, \quad i < N, \\ \ddot{\tilde{p}}_N &= -f(\tilde{p}_N - \tilde{p}_{N-1}) - g(\dot{\tilde{p}}_N - \dot{\tilde{p}}_{N-1}) + w_N. \end{aligned} \quad (7)$$

Note that  $\tilde{p}_0(t) = \dot{\tilde{p}}_0(t) \equiv 0$ , since the reference agent perfectly tracks its desired trajectory. The system can be expressed in the state space form:

$$\dot{x} = \mathbf{f}(x, w), \quad (8)$$

where the state and disturbance vectors are defined as  $x := [\tilde{p}_1, \dot{\tilde{p}}_1, \dots, \tilde{p}_N, \dot{\tilde{p}}_N]^T$  and  $w := [w_1, \dots, w_N]^T$ . The special case  $f(z) = k_0 z$  and  $g(z) = b_0 z$  (where  $z$  is the argument and  $k_0 > 0, b_0 > 0$ ) in the above coupled-ODEs correspond to the case of *linear control* in each architecture. In the case of linear control, the closed-loop can be represented as:

$$\dot{x} = Ax + Bw, \quad (9)$$

where  $A$  is the state matrix that depends on  $k_0, b_0$  and  $B$  is the input matrix with appropriate dimension.

In this paper, we study the stability of the origin  $x = 0$  of the undisturbed system  $\dot{x} = \mathbf{f}(x, 0)$  given in (8) with linear as well as a class of nonlinear controllers for two architectures. In addition, we examine the sensitivity of position tracking errors  $\tilde{p} = [\tilde{p}_1, \dots, \tilde{p}_N]^T$  to the external disturbances  $w = [w_1, \dots, w_N]^T$ .

### 3. STABILITY ANALYSIS

In this section, we present the stability analysis of the origin  $x = 0$  of the undisturbed system  $\dot{x} = \mathbf{f}(x, 0)$  given in (8) with both linear and nonlinear controllers. For the linear case, we also derive formulae showing how the least stable eigenvalue of the state matrix  $A$  in (9) changes with increasing size of the formation. This eigenvalue quantifies the system's convergence rate with respect to initial errors. For the case of non-linear controller, we provide sufficient conditions for asymptotic stability. Since convergence rates for non-linear systems are difficult to obtain analytically, we perform numerical simulations to study the convergence rate with non-linear controllers and compare with corresponding linear controllers. All simulations for studying transient performance correspond to the following scenario: the disturbance acting on each agent is zero; we perturb the initial position of the first agent from its desired value and observe the position tracking error of the last agent  $\tilde{p}_N(t)$ . For the convenience of comparison, we define the following as a measure of transient performance:

$$E := \lim_{T \rightarrow \infty} \frac{1}{x_0^2} \int_0^T \frac{1}{2} k_0 \tilde{p}_N^2(t) + \frac{1}{2} \dot{\tilde{p}}_N^2(t) dt. \quad (10)$$

where  $k_0 > 0$  is the linear position gain given as before and  $x_0$  is the initial error of the first agent:

$$\tilde{p}_1(0) = x_0. \quad (11)$$

The quantity  $E$  is called the *integral of transient energy*. We assume the limit in (10) exists, i.e. the last agent has finite  $\mathcal{L}_2$  energy. In numerical simulations, we use the following estimate of  $E$ ,

$$\hat{E} := \frac{1}{x_0^2} \int_0^T \frac{1}{2} k_0 \tilde{p}_N^2(t) + \frac{1}{2} \dot{\tilde{p}}_N^2(t) dt, \quad (12)$$

where  $T$  is sufficiently large such that all the errors die out. We study through numerical simulations how  $E$  scales with the number of agents  $N$  and the initial error  $x_0$ .

#### 3.1. Stability analysis with linear control

In the statement of the next theorem, the *least stable eigenvalue* of a matrix refers to the eigenvalue with the largest real part.

##### Theorem 1

Consider a 1-D network of  $N$  double-integrator agents with linear control law, i.e.  $f(z) = k_0 z$ ,  $g(z) = b_0 z$ . If  $k_0 > 0, b_0 > 0$ , the closed-loop dynamics are exponentially stable for both the predecessor-following and symmetric bidirectional architectures. Under the same conditions, the following statements hold.

1. With predecessor-following architecture, the least stable eigenvalue of the closed-loop state matrix  $A$  is  $\mu_1 = \frac{-b_0 + \sqrt{b_0^2 - 4k_0}}{2}$ , and this eigenvalue occurs with multiplicity  $N$ .
2. With symmetric bidirectional architecture, when  $N$  is large, the least stable eigenvalue is given by  $\mu_1 = -\frac{\pi^2 b_0}{8N^2} + \Im$ , with multiplicity of 1, where  $\Im$  is an imaginary number.  $\square$

The first statement of the theorem seems to be well known in the community; though we were unable to find a reference for it. The proof of Theorem 1 is given in the appendix.

Although stability guarantees that transients due to initial conditions decay to 0 as  $t \rightarrow \infty$ , the speed at which the transients decay depends quite strongly on the architecture and the controller design. For a linear system, an appropriate measure of this convergence rate is the absolute value of the real part of the least stable eigenvalue of state matrix  $A$ , as long as the least stable eigenvalue is not repeated. If the least stable eigenvalue is repeated, then algebraic growth (peaking) occurs. In that case, the convergence rate is proportional to  $t^k e^{Re(\mu_1)t}$ , where  $k$  is the algebraic multiplicity of the least stable eigenvalue  $\mu_1$ . It follows from Theorem 1 that the real part of the least stable

eigenvalue  $Re(\mu_1)$  in predecessor following architecture is independent of  $N$ , while it decays to 0 with increasing  $N$  for symmetric bidirectional architecture. This makes the predecessor-following architecture appear to have faster convergence rate than the symmetric bidirectional architecture, especially for large  $N$ . However, the large algebraic multiplicity of the least stable eigenvalue in the predecessor-following architecture will cause large algebraic growth of the initial conditions before they decay to 0. Corroboration through numerical simulations is provided in Section 3.3.

### 3.2. Stability analysis with non-linear control

The next two theorems are on the stability of the network with non-linear controllers, their proofs are given in the appendix. In the statements of the theorems that follow we say that a scalar function  $f$  belongs to the sector  $[\varepsilon, K]$  if  $\varepsilon z^2 \leq z f(z) \leq K z^2, \forall z \in \mathbb{R}$ , and it belongs to the sector  $(0, \infty]$  if  $z f(z) > 0, \forall z \neq 0$ .

#### Theorem 2

Consider a 1-D network of double-integrator agents with predecessor-following architecture with controller (3). If  $f, g : \mathbb{R} \rightarrow \mathbb{R}$  satisfy the sector conditions  $f \in [\varepsilon_1, K_1], g \in [\varepsilon_2, K_2]$ , where  $0 < \varepsilon_1 \leq K_1 < \infty, 0 < \varepsilon_2 \leq K_2 < \infty$ , then the origin  $x = 0$  of the undisturbed dynamics  $\dot{x} = \mathbf{f}(x, 0)$  (8) is globally asymptotically stable.  $\square$

#### Theorem 3

Consider a 1-D network of double-integrator agents with symmetric bidirectional architecture with controller (4). If  $f, g : \mathbb{R} \rightarrow \mathbb{R}$  satisfy the sector conditions  $f \in (0, \infty], g \in (0, \infty]$ , then the origin  $x = 0$  of the undisturbed dynamics  $\dot{x} = \mathbf{f}(x, 0)$  (8) is globally asymptotically stable.  $\square$

#### Remark 1

Note that stability with the linear controllers are special cases of Theorem 2 and Theorem 3. Comparing the above two theorems, we notice that the requirement on the sector condition in the predecessor-following architecture is stricter than that of symmetric bidirectional architecture. However, these sector conditions are only sufficient.  $\square$

### 3.3. Numerical comparison between linear and nonlinear controllers for transient decay

Since every practical actuator has saturation limits, saturation-type nonlinearity is of particular interest. The saturation-type nonlinearity in controlling large platoon is practically important and draws many researchers' attention [32, 33]. Throughout this section, we consider the following specific linear and saturation-type nonlinear controllers. The control gain functions  $f(z)$  and  $g(z)$  used in controllers (3) and (4) are given by

$$\begin{aligned} \text{Linear: } f(z) &= k_0 z, & g(z) &= b_0 z, \\ \text{Non-linear: } f(z) &= B_1 \tanh(\gamma_1 z), & g(z) &= B_2 \tanh(\gamma_2 z), \end{aligned} \quad (13)$$

where  $k_0 = 1, b_0 = 0.5, B_1 = 5, \gamma_1 = 0.2, B_2 = 5, \gamma_2 = 0.1$ . The parameters have been chosen in such a way that the slopes of  $f(z)$  or  $g(z)$  near the origin are equal to  $k_0$  and  $b_0$ , respectively. This is done to make the linear and non-linear cases comparable to some extent. Note that these  $f(z)$  and  $g(z)$  do not satisfy the sector conditions assumed in Theorem 2 globally, but only satisfy the sector conditions locally. However, the region in which they satisfy the sector condition can be made arbitrarily large by choosing sufficiently small  $\varepsilon_1$  and  $\varepsilon_2$ .

We compare the convergence rate and transient performance between linear and nonlinear controllers through numerical simulations. Figure 2 (a) depicts the transients of the 1-D network with linear and nonlinear controllers for predecessor-following architecture. The algebraic growth for linear controller which is predicted by Theorem 1 is observed. We also see that the nonlinear controller has much smaller peak error than the linear controller. The transients in the symmetric bidirectional architecture are shown in Figure 2 (b). We see that (i) the performance of the non-linear case is similar to that of the linear controller, and (ii) the peak value of the error is much smaller compared to that in the predecessor-following architecture, no matter the controller is linear or nonlinear.

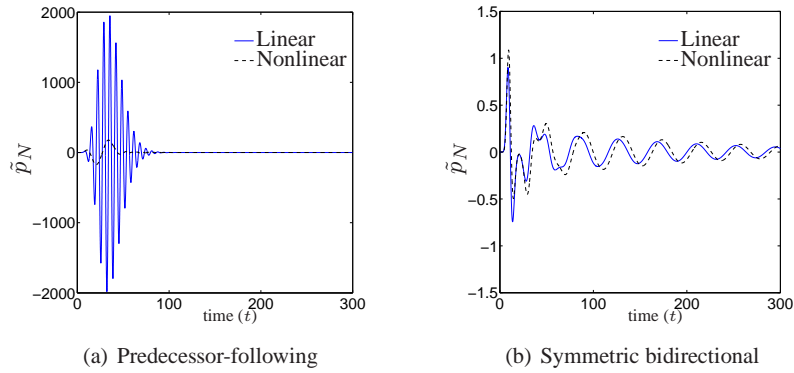


Figure 2. Comparison of transients of the position tracking error of the last agent for a network of  $N = 10$  agents between linear and nonlinear controller. The initial condition of the first agent used is  $x_0 = 10$ .

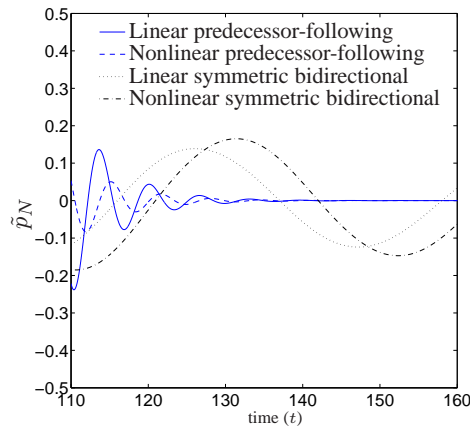


Figure 3. Comparison of convergence rate for a network of  $N = 10$  agents between predecessor-following and symmetric bidirectional architectures. The initial condition of the first agent used is  $x_0 = 10$ .

Figure 3 shows a “zoomed-in” version of the transient response. We see from the figure that the convergence rates of the linear and non-linear controllers in each architecture are similar. In addition, the error in the predecessor-following architecture is smaller than in the case of symmetric bidirectional architecture for *large t*. This can be explained in the linear case from the real part of the least stable eigenvalue: it is much larger in the predecessor-following architecture compared to the symmetric bidirectional architecture,  $O(1)$  vs.  $O(1/N^2)$  (recall Theorem 1). The similarity between the simulation results in the non-linear and linear cases indicate that the convergence rate in the predecessor-following architecture is higher than that in the symmetric bidirectional one, whether control is linear or nonlinear.

Figure 4 and Figure 5 show the estimate of energy measure  $\hat{E}$  for  $T = 10^4$  seconds (defined in (12)) as a function of  $N$  and  $x_0$  respectively. Recall  $x_0$  is the initial position error of the first agent, it’s given in (11). We see that (i) the energy in the predecessor-following architecture has a much worse scaling trend with  $N$  or  $x_0$  than that in symmetric bidirectional architecture, no matter the controller is linear or nonlinear, (ii) nonlinear controller performs better than linear controller in the predecessor-following architecture (Figure 4 (a), Figure 5 (a)), whereas it performs similarly or worse in the symmetric bidirectional architecture (Figure 4 (b), Figure 5 (b)).



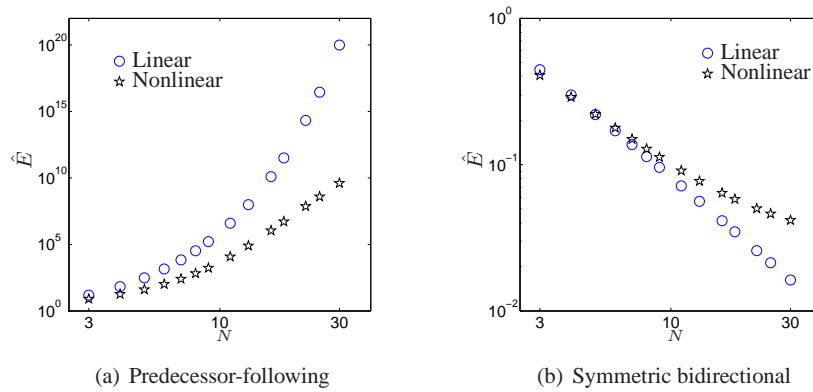


Figure 4. Comparison of  $\hat{E}$  between linear and nonlinear controllers as a function of  $N$ . The measure  $E$  is estimated by numerically evaluating the integral in (12) for  $T = 10^4$  s. The initial condition of the first agent used is  $x_0 = 10$ .

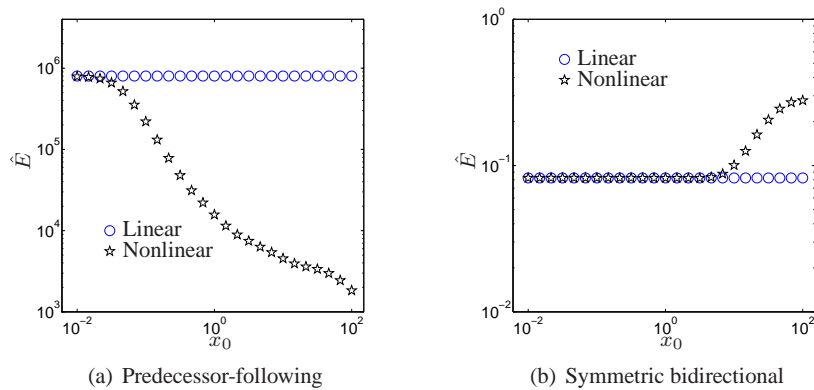


Figure 5. Comparison of  $\hat{E}$  between linear and nonlinear controllers for a network of  $N = 10$  agents as a function of initial conditions  $x_0$ . The measure  $\hat{E}$  is estimated by numerically evaluating the integral in (12) for  $T = 10^4$  s.

Table I. Comparison of transient performances between the two architectures.

	predecessor-following	symmetric bidirectional
convergence rate	good	bad
transient energy	bad	good

Table II. Comparison of transient performances between linear and nonlinear controllers.

	linear controller	nonlinear controller
predecessor-following	bad	good
symmetric bidirectional	good	bad

### 3.4. Design guidelines based on transient response

Based on the numerical and analytical results, the comparisons of performance are summarized in Table I and Table II. It follows that the predecessor-following architecture has a faster convergence rate (good) but much higher *integral of transient energy*  $E$  (bad) compared to the symmetric bidirectional architecture. These conclusions hold irrespective of whether the controller is linear or nonlinear, see Figure 2-5. In fact the transients are so large with the predecessor-following architecture that it is very likely to lead to collisions even for small initial errors. So if a design choice is to be made among the two architectures, the symmetric bidirectional should be chosen. Within the bidirectional architecture, the linear controller seems to perform slightly better than the nonlinear one, so the linear controller should be chosen. If for some reason the predecessor-following architecture has to be used, the non-linear control law should be used since it clearly outperforms the linear one in terms of transient energy.

## 4. ROBUSTNESS (SENSITIVITY TO EXTERNAL DISTURBANCES)

In this section, we study the sensitivity of the network to external disturbances. Specifically, we examine appropriate gains from (i) a disturbance on the first agent  $w_1 \in \mathbb{R}$  to the position tracking error of the last agent  $\tilde{p}_N \in \mathbb{R}$ , and (ii) disturbances acting on all agents  $w \in \mathbb{R}^N$  to the position tracking errors of all agents  $\tilde{p} \in \mathbb{R}^N$ . Both sinusoidal and random disturbances are considered. For the first scenario, we consider the metric *first-to-last amplification factor* ( $A_{FTL}$ ), defined as the  $L_2$  gain from input  $w_1$  to output  $\tilde{p}_N$ :

$$A_{FTL}^{linear \text{ or } nonlinear} = \sup \frac{\|\tilde{p}_N\|_{\mathcal{L}_2(\tau)}}{\|w_1\|_{\mathcal{L}_2(\tau)}}, \quad (14)$$

where the  $\mathcal{L}_2$  norm in the expression above is defined in the extended space [34], i.e.  $\|e\|_{\mathcal{L}_2(\tau)} := \sqrt{\int_0^\tau \|e(t)\|^2 dt}$  for a large but finite  $\tau$ . In the linear case, denoting by  $G_{FTL}(s)$  the SISO transfer function from  $w_1$  to  $\tilde{p}_N$ , this is the same as the  $H_\infty$  norm of  $G_{FTL}(s)$  [34], i.e.,

$$A_{FTL}^{linear} = \max_{\omega} |G_{FTL}(j\omega)| = |G_{FTL}(j\omega_p)|, \text{ where } \omega_p := \arg \max_{\omega} |G_{FTL}(j\omega)|, \quad (15)$$

where we have assumed for the moment that the maximum is achieved at a finite frequency. The justification will be provided later. In the non-linear case we use the following quantity as a conservative estimate of the amplification factor:

$$\hat{A}_{FTL}^{nonlinear} = \frac{\|\tilde{p}_N\|_{\mathcal{L}_2(\tau)}}{\|w_1\|_{\mathcal{L}_2(\tau)}}, \quad (16)$$

where  $w_1 = a_1 \sin(\omega_p t)$ ,  $a_1$  is a positive constant, and  $\omega_p$  is the peak frequency for the linear case that is defined in (15).

For the second scenario (effect of disturbances acting on every agent on their position tracking errors), we define the *all-to-all amplification factor*  $A_{ATA}$  as the  $L_2$  gain from the vector of disturbances  $w(t) = [w_1(t), \dots, w_N(t)]$  to position tracking error vector  $\tilde{p}(t) = [\tilde{p}_1(t), \dots, \tilde{p}_N(t)]$ :

$$A_{ATA}^{linear \text{ or } nonlinear} = \sup \frac{\|\tilde{p}\|_{\mathcal{L}_2(\tau)}}{\|w\|_{\mathcal{L}_2(\tau)}}, \quad (17)$$

In the linear case this is the  $H_\infty$  norm of the MIMO transfer function  $G_{ATA}(s)$  from  $w$  to  $\tilde{p}$ .

$$A_{ATA}^{linear} = \max_{\omega} \sigma_{\max}(G_{ATA}(j\omega)) = \sigma_{\max}(G_{ATA}(j\omega_p)),$$

where we have assumed the maximum is achieved,  $\omega_p := \arg \max_{\omega} \sigma_{\max}(G_{ATA}(j\omega))$  and  $\sigma_{\max}$  denotes the maximum singular value. In the non-linear case, evaluating  $A_{ATA}^{nonlinear}$  is intractable, so

we use following conservative estimate:

$$\hat{A}_{ATA}^{nonlinear} := \frac{\|\tilde{p}\|_{\mathcal{L}_2(\tau)}}{\|w\|_{\mathcal{L}_2(\tau)}}, \quad (18)$$

where  $w = [a_1 \sin(\omega_p t + \theta_1), \dots, a_N \sin(\omega_p t + \theta_N)]$  and  $a = [a_1, \dots, a_N]$ ,  $\theta = [\theta_1, \dots, \theta_N]$  are the parameters that achieve the  $\mathcal{L}_2$  norm in the linear case. The choice of these parameters is given in Theorem 4 and Corollary 1. Note from (14), (16) and (17), (18) that the estimates for the non-linear case are lower bounds:  $\hat{A}_{FTL}^{nonlinear} \leq A_{FTL}^{nonlinear}$  and  $\hat{A}_{ATA}^{nonlinear} \leq A_{ATA}^{nonlinear}$ .

We also examine the effect of random disturbances. Specifically, let  $w(t)$  in the closed-loop dynamics (8) be a scalar (or vector) of white noise with zero mean and autocorrelation function  $E[w(t)w(t+\tau)^T] = \sigma_0 \delta(\tau)I, \forall t, \forall \tau$ , where  $\sigma_0$  is a constant,  $\delta(\tau)$  is the Dirac delta function and  $I$  is the identity matrix with appropriate dimension. Similar to sinusoidal disturbances, we define the following two metrics (i) *first-to-last ratio* and (ii) *all-to-all ratio*:

$$R_{FTL}^{linear \text{ or } nonlinear} := \lim_{t \rightarrow \infty} \frac{\sqrt{E(\tilde{p}_N^2(t))}}{\sigma_0}, \quad R_{ATA}^{linear \text{ or } nonlinear} := \lim_{t \rightarrow \infty} \frac{\sqrt{E(\tilde{p}(t)^T \tilde{p}(t))}}{\sigma_0}, \quad (19)$$

where  $E(\cdot)$  denotes the expected value and we have assumed the above limits exist. Notice in the linear case, the above ratios are exactly the  $H_2$  norms of the appropriate transfer functions from the white noise disturbances to the position tracking errors. The steady-state covariance matrix of the state  $\tilde{p}(t)$  of the system (9) that is driven by a white noise process  $w(t)$  is given by solution  $P$  of the following Lyapunov equation [35, Chapter 4]:

$$AP + PA^T = -Q,$$

where  $Q = \sigma_0 BB^T$ , and  $B$  is the appropriate input matrix given in (9). Since  $A$  is Hurwitz, it guarantees the limit in (19) exists [35]. The steady-state expectations  $E(\tilde{p}_N^2(t))$  and  $E(\tilde{p}(t)^T \tilde{p}(t))$  given in (19) can be obtained by extracting the second last diagonal entry of  $P$  and summing the odd diagonal entries of  $P$  respectively, which yields

$$R_{FTL}^{linear} = \frac{\sqrt{P(2N-1, 2N-1)}}{\sigma_0}, \quad R_{ATA}^{linear} = \frac{\sqrt{\sum_{i=1}^N P(2i-1, 2i-1)}}{\sigma_0}. \quad (20)$$

It should be pointed out that these results are not as analytical as the results in [29, 36, 30]. Our study of random disturbances with linear control is closely related to the works by Bamieh, Jovanovic and their coworkers [29, 30]. They derived scaling laws of all-to-all ratio for both predecessor-following and symmetric bidirectional architecture, which are similar to the scaling laws of  $H_\infty$  norms established in this paper, see Remark 2 for more details.

For the non-linear controllers as well as linear controllers, we use the following estimate of the ratio defined in (19), which can be computed from simulation data:

$$\hat{R}_{FTL}^{linear \text{ or } nonlinear} := \frac{\sqrt{E(\tilde{p}_N^2(T))}}{\sigma_0}, \quad \hat{R}_{ATA}^{linear \text{ or } nonlinear} := \frac{\sqrt{E(\tilde{p}(T)^T \tilde{p}(T))}}{\sigma_0}, \quad (21)$$

where  $T$  is sufficiently large such that the transients die out. Monte-Carlo simulations are used to estimate the first-to-last and all-to-all ratios. For example, to compute the first-to-last ratio for the predecessor-following architecture with nonlinear controller, the noise-driven system (6) is converted into a standard stochastic differential equation (SDE) form

$$\begin{aligned} d\tilde{p}_1 &= \dot{\tilde{p}}_1 dt, & d\dot{\tilde{p}}_1 &= -f(\tilde{p}_1)dt - g(\dot{\tilde{p}}_1)dt + \sigma_0 dW(t), \\ d\tilde{p}_i &= \dot{\tilde{p}}_i dt, & d\dot{\tilde{p}}_i &= -f(\tilde{p}_i - \tilde{p}_{i-1})dt - g(\dot{\tilde{p}}_i - \dot{\tilde{p}}_{i-1})dt, \end{aligned} \quad (22)$$

where  $W(t)$  is a standard Wiener process. Sample paths of the states are computed by using Euler-Maruyama Method to numerically integrate the SDE (22) [37]. The metric  $\hat{R}_{FTL}^{nonlinear}$  is now estimated by performing appropriate averaging over a large number of simulations, after letting each simulation proceed sufficiently long to allow transients to die out.

#### 4.1. Sensitivity to disturbance with linear control

As stated earlier, analytical results on the sensitivity to disturbances are possible only for the linear case. The first result is on the sensitivity of the predecessor-following architecture with linear control.

##### Theorem 4

Consider a 1-D network of  $N$  double-integrator agents with predecessor-following architecture. With linear controller  $f(x) = k_0x$  and  $g(x) = b_0x$  in (3), the first-to-last amplification  $A_{FTL}^{linear}$  and all-to-all amplification  $A_{ATA}^{linear}$  satisfy

$$\beta_1\alpha^{N-1} \leq A_{FTL}^{linear} \leq \beta_2\alpha^{N-1}, \quad \beta_1\alpha^{N-1} \leq A_{ATA}^{linear} \leq \frac{\beta_2(\alpha^N - 1)}{\alpha - 1},$$

where  $\alpha = |T(j\omega_T)| > 1$ ,  $\beta_1 = |S(j\omega_T)|$  and  $\beta_2 = |S(j\omega_S)|$ , in which  $T(s) = \frac{b_0s+k_0}{s^2+b_0s+k_0}$ ,  $S(s) = \frac{1}{s^2+b_0s+k_0}$ , and  $\omega_T$  and  $\omega_S$  are the peak frequencies of  $T(s)$  and  $S(s)$  respectively.

Furthermore, when  $N \gg 1$ ,

$$A_{FTL}^{linear} \approx \beta_1\alpha^{N-1}, \quad A_{ATA}^{linear} \approx \beta_1\sqrt{\frac{(\alpha^{2N} - 1)}{\alpha^2 - 1}}, \quad \omega_p \approx \frac{\sqrt{\sqrt{k_0^4 + 2k_0^3b_0^2} - k_0^2}}{b_0}. \quad (23)$$

Moreover, a sufficient condition for a disturbance  $w = [w_1, \dots, w_N] = [a_1 \sin(\omega t + \theta_1), \dots, a_N \sin(\omega t + \theta_N)]$  to yield the worst amplification factors is  $a = [a_1, \dots, a_N] = [a_1, 0, \dots, 0]$ , where  $a_1$  is an arbitrary constant and  $\omega = \omega_p$ ,  $\theta = [\theta_1, \dots, \theta_N] = 0$ .  $\square$

The proof of this theorem is omitted here, since it is similar to the proof of Lemma 1 in [14]. The interested reader can find a detailed proof in [38].

The next theorem is the corresponding result for the symmetric-bidirectional architecture.

##### Theorem 5

Consider a 1-D network of  $N$  double-integrator agents with symmetric bidirectional architecture. With linear controller  $f(x) = k_0x$  and  $g(x) = b_0x$  in (4), the first-to-last and all-to-all amplifications satisfy

$$\left(\frac{16}{\pi^3 b_0 \sqrt{k_0}}\right)N \leq A_{FTL}^{linear} \leq \left(\frac{\pi^3 + 18\pi}{12b_0\sqrt{2k_0}}\right)N, \quad \text{when } N \gg 1,$$

$$\left(\frac{1}{b_0\sqrt{k_0}\pi^3}\right)(2N+1)^3 \leq A_{ATA}^{linear} \leq \left(\frac{1}{4b_0\sqrt{2k_0}}\right)(2N+1)^3, \quad \forall N.$$

Furthermore, when  $N \gg 1$ , the all-to-all amplification and its peak frequency are asymptotically

$$A_{ATA}^{linear} \approx \frac{8N^3}{\sqrt{k_0}b_0\pi^3}, \quad \omega_p \approx \frac{\sqrt{k_0}\pi}{2N}. \quad \square$$

The asymptotic formulae for the first-to-last amplification and its peak frequency with symmetric bidirectional architecture are conjectured as follows. The argument for the conjecture is given in the end of appendix.

##### Conjecture 1

Assume the conditions of Theorem 5 hold. When  $N \gg 1$ , the first-to-last amplification and the peak frequency of the 1-D network are asymptotically

$$A_{FTL}^{linear} \approx \frac{8N}{\sqrt{k_0}b_0\pi^2}, \quad \omega_p = \omega_1 \approx \frac{\sqrt{k_0}\pi}{2N}. \quad \square$$

The following result is a corollary of Theorem 5, it provides sufficient conditions for an input to achieve the  $\mathcal{L}_2$  gain in the all-to-all scenario.

Table III. Comparison of robustness performances between the two architectures.

	predecessor-following	symmetric bidirectional
first-to-last amplification	bad ( $O(\alpha^N)$ , $\alpha > 1$ )	good ( $O(N)$ )
all-to-all amplification	bad ( $O(\alpha^N)$ , $\alpha > 1$ )	good ( $O(N^3)$ )

Table IV. Comparison of robustness performances between linear and nonlinear controllers.

	linear controller	nonlinear controller
predecessor-following	bad	good
symmetric bidirectional	good	bad

### Corollary 1

Assume the conditions of Theorem 5 hold, if the disturbance input satisfies  $w = [w_1, \dots, w_N] = v_1 \sin(\omega_1 t)$ , where  $v_1$  and  $\omega_1$  are given in (34) and (38) respectively, are the eigenvector and the peak frequency corresponding to the principal eigenvalue  $\lambda_1$  of  $L$  given in (32), then

$$A_{ATA}^{linear} = \frac{\|\tilde{p}\|_{\mathcal{L}_2(\tau)}}{\|w\|_{\mathcal{L}_2(\tau)}}. \quad \square$$

The above corollary indicates that a sufficient condition for a disturbance  $w = [w_1, \dots, w_N] = [a_1 \sin(\omega t + \theta_1), \dots, a_N \sin(\omega t + \theta_N)]$  to yield the all-to-all amplification factor for the symmetric bidirectional architecture is  $a = [a_1, \dots, a_N] = v_1$ ,  $\omega = \omega_1$  and  $\theta = [\theta_1, \dots, \theta_N] = 0$ . This result will be used to compute the estimate of all-to-all amplification factor  $\hat{A}_{ATA}^{nonlinear}$  for nonlinear controllers, which is defined in (14).

### Remark 2

Based on the analytical results in Theorem 4 and Theorem 5 (and Conjecture 1), we summarize the robustness results in Table III. We observe that symmetric bidirectional architecture has much better robustness than predecessor-following architecture. In particular, the first-to-last amplification scales geometrically in  $N$  as  $O(\alpha^N)$ ,  $\alpha > 1$  for predecessor-following architecture but only linearly in  $N$  as  $O(N)$  for symmetric bidirectional architecture. The all-to-all amplification scales as  $O(\alpha^N)$  for predecessor-following architecture while as  $O(N^3)$  for symmetric bidirectional architecture. Similar to the results on  $H_\infty$  norms established in this paper, it's worthy to mention that with predecessor-following architecture, the "all-to-all" ratio/ $H_2$  norm of the 1-D network also scales exponentially with the number of agents  $N$ , even with absolute velocity feedback [30], whereas we consider in this paper the relative velocity feedback case. For the symmetric bidirectional architecture, Bamieh et al. showed in [29] that the "all-to-all" ratio/ $H_2$  norm scales only as  $O(N^3)$ .  $\square$

### 4.2. Numerical comparison of sensitivity to disturbances between linear and nonlinear controllers

In this section, we present robustness metrics of the 1-D network with linear and nonlinear controllers empirically estimated using numerical computations. The analytical predictions of the performance metrics for the linear controllers are also presented to verify these predictions. The controllers used are the ones given by (13).

Figure 6 shows the first-to-last amplification factor as a function of  $N$ : Figure 6 (a) is for predecessor following and Figure 6 (b) is for symmetric bidirectional. The following observations are made. (i) The lower and upper bounds and asymptotic formulae derived are quite accurate, especially for the predecessor following case. For the symmetric bidirectional architecture,

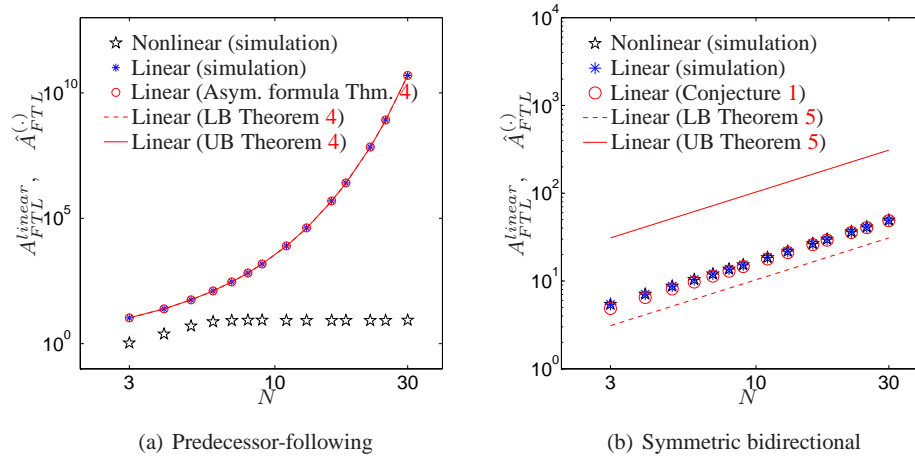


Figure 6. First-to-last amplification: sinusoidal disturbances. Comparison of first-to-last amplification factor with linear and nonlinear controllers. The sinusoidal disturbance on the first agent used is  $0.1 \sin(\omega_p t)$ . LB and UB stands for “lower bound” and “upper bound”.

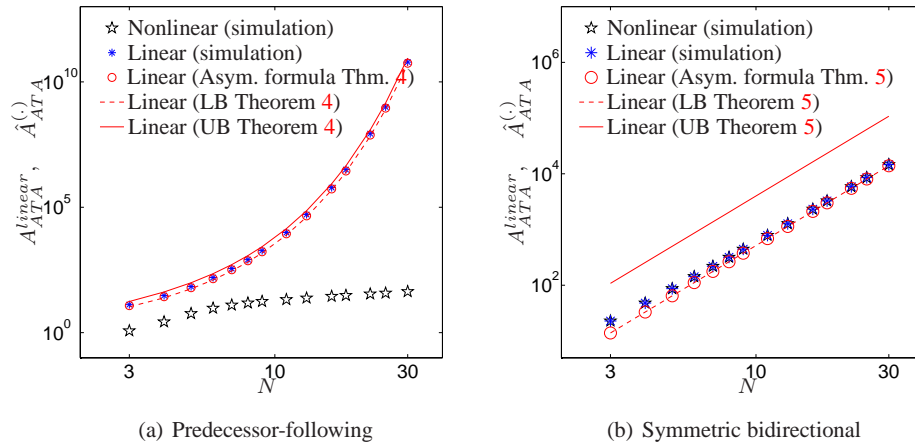


Figure 7. All-to-all amplification: sinusoidal disturbances. Comparison of all-to-all amplification factor with linear and nonlinear controllers. The sinusoidal disturbances used is  $v_1 \sin(\omega_p t)$ , where  $v_1$  is the first eigenvector of  $L$  given in (34). LB and UB stands for “lower bound” and “upper bound”.

Conjecture 1 is quite accurate. (ii) In the predecessor-following architecture, the growth of the first-to-last amplification factor with respect to  $N$  is much slower with the nonlinear controller than with the linear controller, as readily seen in Figure 6 (a). In the symmetric bidirectional architecture, there is little difference between the two controllers for this sinusoidal disturbance, as seen from Figure 6 (b). (iii) Comparing Figure 6 (a) and (b) we see that the symmetric bidirectional architecture has a much smaller first-to-last amplification factor than the predecessor-following architecture, when the controller is linear. However, when nonlinear controller is applied, the symmetric bidirectional architecture has a slightly worse scaling trend than that of the predecessor-following case. The same conclusions can be drawn to the case of all-to-all amplification factor, whose numerical results are shown in Figure 7.

To examine the effect of random disturbances, we compute the estimate  $\hat{R}$  that is defined in (21) for  $T = 3000$  seconds, through Monte-Carlo simulations for both linear and non-linear cases. For the first-to-last ratio, Figure 8 shows  $\hat{R}_{FTL}$  vs.  $N$  for a fixed  $\sigma_0$  while Figure 9 shows  $\hat{R}_{FTL}$  vs.  $\sigma_0$ , the strength of the noise, for a fixed  $N$ . Numerical and analytical (Eq. (20)) results on the all-to-all ratio are shown in Figure 10 and Figure 11. The conclusion of robustness to random noise

drain from Figure 8-11 are the same as that for robustness to sinusoidal disturbances, we omit the discussion due to space limit.

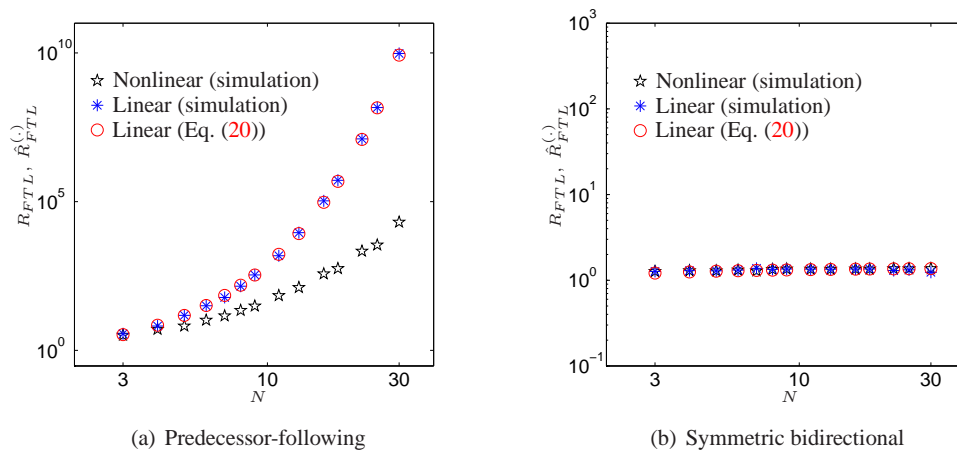


Figure 8. First-to-last ratio: random disturbance ( $\sigma_0 = 1$ ), for both linear and non-linear controllers.

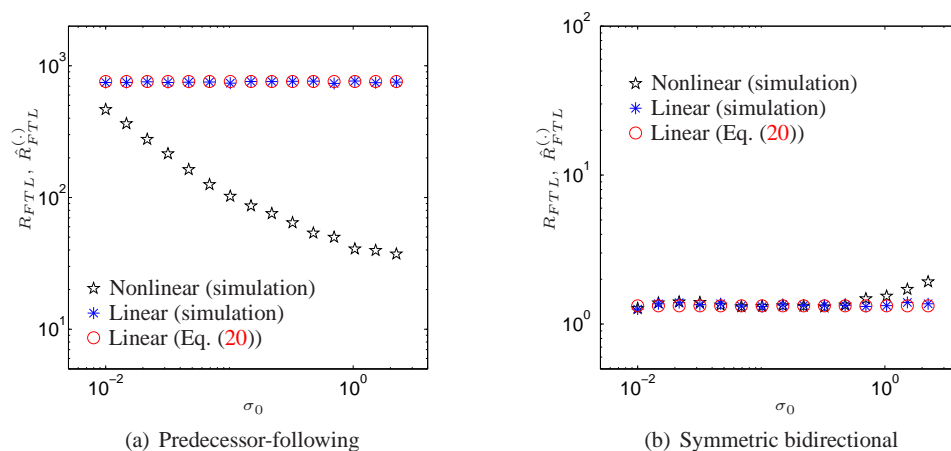


Figure 9. First-to-last ratio: random disturbances. Comparison of the ratios  $R_{FTL}, \hat{R}_{FTL}$  of a network of 10 agents as a function of the standard deviation  $\sigma_0$  of the white noises.

#### 4.3. Design guidelines based on robustness

Based on the empirical as well as the analytical results, the robustness performance results are summarized in Tale III and Table IV. A few broad conclusions can be arrived at that are useful for making design choices: (i) by comparing part (a) with part (b) for Figures 8-11 we conclude that the predecessor following architecture has poorer performance compared to the symmetric bidirectional one, and the difference gets more pronounced as  $N$  increases. Moreover, this conclusion holds irrespective of whether the disturbance is sinusoidal or random, and whether the first-to-last ratio or the all-to-all ratio is used as a metric of robustness; (ii) If symmetric bidirectional architecture is indeed used, both the linear and non-linear control laws have almost identical robustness. The only exception is when the strength of the disturbance is large, in which case the non-linear control law performs poorly compared to the linear one. Thus, a designer can use the linear control law due to simplicity without losing performance. Since, actuator saturation will be present in practice,

the resulting closed loop system even with a linear control law will be closer to the non-linear system studied here. The previous observation therefore tells us that the symmetric bidirectional architecture is robust to modeling errors as well and therefore preferable from a practical standpoint; (iii) If the predecessor architecture is to be used due to other constraints such as cost, the non-linear control law has better robustness to disturbance than its linear counterpart; see part (a) of Figure 8-11. Therefore, in this case the non-linear controller should be used.

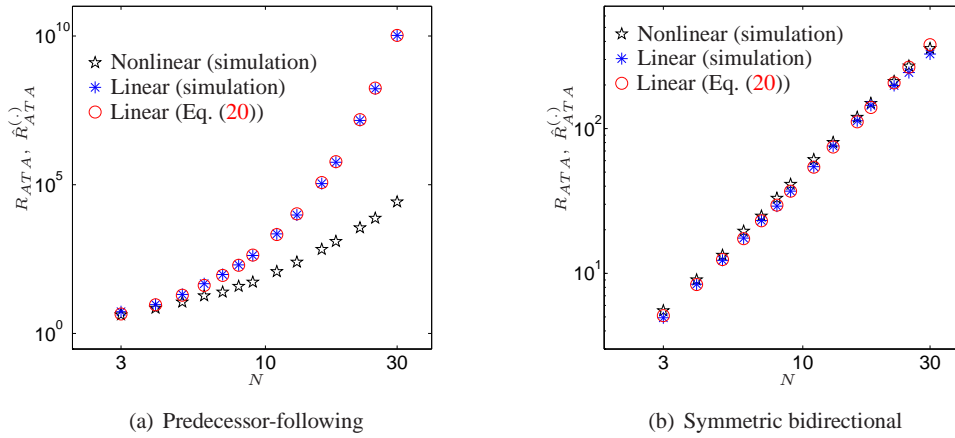


Figure 10. All-to-all ratio: random disturbances. Comparison of the ratios  $R_{ATA}$ ,  $\hat{R}_{ATA}$  as a function of the number of agents  $N$  with white noise disturbances. The value of  $\sigma_0$  used is 1.

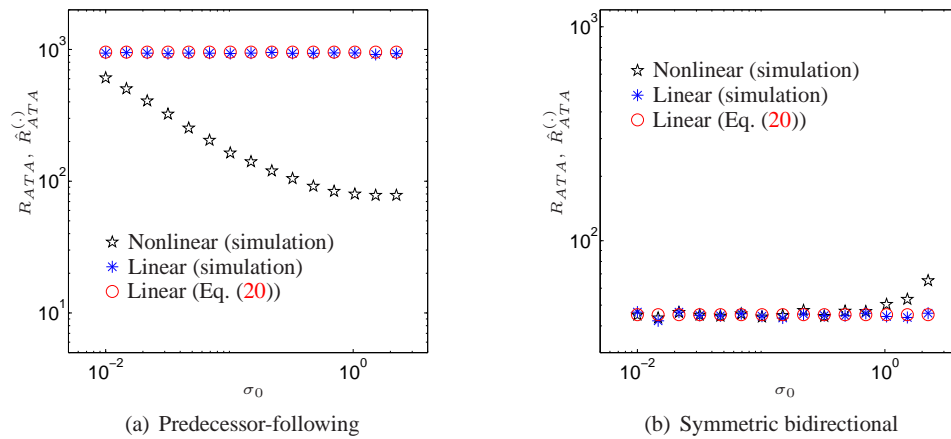


Figure 11. All-to-all ratio: random disturbances. Comparison of the ratios  $R_{ATA}$ ,  $\hat{R}_{ATA}$  of a platoon of 10 agents as a function of the standard deviation  $\sigma_0$  of the white noises.

## 5. SUMMARY

We studied the stability and robustness of large 1-D networks of double-integrator agents for two different decentralized architectures: predecessor following and symmetric bidirectional. Both linear and nonlinear controllers with certain sector non-linearities were examined. For the linear



case, we obtained exact formulae for convergence rates of the closed loop, while for the non-linear case, closed loop stability was proved. It was shown that the predecessor-following architecture with linear control has much faster convergence rate than the symmetric bidirectional architecture, but it suffers from high algebraic growth of initial errors. To compare performance with the non-linear controller for which convergence rate could not be computed, a “integral of transient energy” measure was proposed. Simulations showed that the symmetric bidirectional architecture has a better transient performance than the predecessor following one, whether the controller is linear and non-linear.

The robustness (sensitivity to external disturbances) of the closed loop is studied through two metrics - called the first-to-last amplification factor and all-to-all amplification factor (called ratios instead of amplification factors when the disturbance is random instead of sinusoidal). In case of linear control, we derived scaling laws of the amplification factors of the 1-D network with respect to the number of agents for both architectures. For the nonlinear control case, the amplification factors were examined by extensive numerical simulations. The overall conclusion derived from a mix of analysis and simulations was that the symmetric bidirectional architecture’s performance scales with  $N$  much better than that of the predecessor-following architecture. Simulations show that in case of the predecessor-following architecture, a class of saturation-type nonlinear controllers perform better compared to the linear control, both in terms of transient performance and sensitivity to external disturbances.

It should be noticed that the conclusions - and design guidelines - drawn from robustness considerations are consistent with the design guidelines drawn purely from transient response considerations; cf. Section 4.3 and Section 3.4. Another important conclusion of these studies is the following: architecture has a more profound impact on performance than linearity or non-linearity of the plant dynamics/control. The symmetric bidirectional architecture is seen to perform better than the predecessor-following architecture in almost all cases, with linear or non-linear control, for various metrics of performance, and with sinusoidal or random disturbance. The only exception is convergence rate. Everything else being equal, the predecessor-following architecture has a faster convergence rate than the symmetric bidirectional. However, this comes with the associated cost of higher peak transients and higher transient energy, so that with the predecessor-following architecture, collisions between agents can be avoided only if the initial spacial errors are extremely small.

Some of the simplifying assumptions made in the paper for the ease of exposition can be removed without much technical difficulty. Here we have limited ourselves to a *homogeneous* network: each agent in the network has the same open-loop dynamics and uses the same control law. Convergence rate results in the linear case remain the same asymptotically (for large  $N$ ) even in the case of a *heterogeneous* network, in which the masses and control gains vary from one agent to another. It was shown in [39] that in the linear symmetric bidirectional case, heterogeneity in agent masses and control gains do not affect the asymptotic scaling (with  $N$ ) of the convergence rate, they only change the coefficient. The non-linear stability analysis in this paper can also be extended in a straightforward manner to the heterogeneous network. The linear stability results of this paper can be extended to formations with more general information graphs - compared to the 1-D formation studied here - by using the methodology of [38, 40].

The scaling laws for the convergence rate and robustness metrics for the linear case can also be extended to more general class of agent models and dynamic compensators. In particular, when the agent model  $H(s)$  (transfer function from input to position) is not simply  $1/s^2$  but  $1/s^2 P(s)$  where  $P(s)$  is a transfer function with  $0 < P(0) < \infty$ , the analysis can be carried out in a manner similar to that in [14] for the predecessor following case and [23] for the symmetric bidirectional case. As shown in [23], the key attribute of the model that determines robustness scaling is the number of integrators in the loop, additional dynamics only affect the high frequency portion while the robustness scaling with  $N$  is determined only by the low frequency portion of the frequency response of the loop transfer function. The reason for the importance of the low frequency band is the unbounded gain and  $-180^\circ$  phase of  $1/s^2$  at dc. As a result the worst-case amplification occurs

at a progressively lower frequency as  $N$  increases. Recall Theorem 5: the peak frequencies for the symmetric bidirectional case is  $O(1/N)$ .

It should be emphasized that the results for the symmetric architecture obtained here do not extend to the *asymmetric* case, in which an agent uses information from its predecessor (front-neighbor) differently than the information from its follower (back neighbor). One can introduce a *mistuning parameter*  $\epsilon \in [-1, 1]$  to quantify this asymmetry:  $\epsilon = 0$  corresponds to the case of symmetric bidirectional case while  $\epsilon = 1$  corresponds to the predecessor following architecture, with  $0 < \epsilon < 1$  corresponding to a case when the front neighbor's information is weighted more heavily than that of the back neighbor, and  $-1 < \epsilon < 0$  corresponding to the opposite. The difference between the two architectures established here already provides evidence that asymmetry has a non-negligible effect. Recent works have shown that even small amount of asymmetry can have a huge impact, on both convergence rate [41, 39] and robustness in terms of, respectively,  $H_\infty$  norm [28] and  $H_2$  norm [30]. It was shown in [39, 28, 30] that asymmetry can either significantly improve or deteriorate the system's convergence rate and robustness, depends on the choice of asymmetry. These works have studied the linear case. Analysis of stability with general asymmetric non-linear control is an open problem. In fact, analysis of the sensitivity to disturbance with general asymmetric control (linear or non-linear) is also an open problem.

#### REFERENCES

1. Hedrick JK, Tomizuka M, Varaiya P. Control issues in automated highway systems. *IEEE Control Systems Magazine* December 1994; **14**:21–32, doi:10.1109/37.334412.
2. Ioannou P. *Automated Highway Systems*. Plenum Pub Corp, 1997.
3. Tanner H, Christodoulakis D. Decentralized cooperative control of heterogeneous vehicle groups. *Robotics and autonomous systems* 2007; **55**(11):811–823.
4. Hoffman T. GRAIL: Gravity mapping the moon. *IEEE Aerospace conference*, 2009; 1–8, doi:10.1109/AERO.2009.4839327.
5. Okubo A. Dynamical aspects of animal grouping: swarms, schools, flocks, and herds. *Advances in Biophysics* 1986; **22**:1–94.
6. Ioannou P, Chien C. Autonomous intelligent cruise control. *Vehicular Technology, IEEE Transactions on* 1993; **42**(4):657–672.
7. Ioannou P, Xu Z, Eckert S, Clemons D, Sieja T. Intelligent cruise control: theory and experiment. *Decision and Control, 1993., Proceedings of the 32nd IEEE Conference on*, IEEE, 1993; 1885–1890.
8. Bjornberg A. Autonomous intelligent cruise control. *Vehicular Technology Conference, 1994 IEEE 44th*, IEEE, 1994; 429–433.
9. Darbha S, Rajagopal K. Intelligent cruise control systems and traffic flow stability. *Transportation Research Part C: Emerging Technologies* 1999; **7**(6):329–352.
10. Darbha S, Hedrick JK. String stability of interconnected systems. *IEEE Transactions on Automatic Control* March 1996; **41**(3):349–356.
11. Darbha S, Hedrick J, Chien C, Ioannou P. A comparison of spacing and headway control laws for automatically controlled vehicles. *Vehicle System Dynamics* 1994; **23**(8):597–625.
12. Zhang Y, Kosmatopoulos EB, Ioannou PA, Chien CC. Autonomous intelligent cruise control using front and back information for tight vehicle following maneuvers. *IEEE Transactions on Vehicular Technology* January 1999; **48**:319–328.
13. Klinge S, Middleton R. Time headway requirements for string stability of homogeneous linear unidirectionally connected systems. *Proceedings of the 48th IEEE Conference on Decision and Control*, IEEE, 2009; 1992–1997.
14. Seiler P, Pant A, Hedrick JK. Disturbance propagation in vehicle strings. *IEEE Transactions on Automatic Control* October 2004; **49**:1835–1841.
15. Lestas I, Vinnicombe G. Scalability in heterogeneous vehicle platoons. *American Control Conference*, 2007; 4678–4683.
16. Liu X, Goldsmith A, Mahal S, Hedrick J. Effects of communication delay on string stability in vehicle platoons. *Intelligent Transportation Systems, 2001. Proceedings. 2001 IEEE*, IEEE, 2001; 625–630.
17. Peppard L. String stability of relative-motion PID vehicle control systems. *Automatic Control, IEEE Transactions on* 1974; **19**(5):579–581.
18. Chu K. Decentralized control of high-speed vehicular strings. *Transportation Science* 1974; **8**(4):361.
19. Stotsky A, Chien C, Ioannou P. Robust platoon-stable controller design for autonomous intelligent vehicles. *Proceedings of the 33rd IEEE Conference on Decision and Control*, vol. 3, IEEE, 1994; 2431–2436.
20. Bose A, Ioannou P. Environmental evaluation of intelligent cruise control (icc) vehicles. *Intelligent Transportation Systems, 2000. Proceedings. 2000 IEEE*, IEEE, 2000; 352–357.
21. Middleton R, Braslavsky J. String instability in classes of linear time invariant formation control with limited communication range. *IEEE Transactions on Automatic Control* 2010; **55**(7):1519–1530.
22. Khatir ME, Davison EJ. Decentralized control of a large platoon of vehicles using non-identical controllers. *Proceedings of the 2004 American Control Conference*, 2004; 2769–2776.

23. Barooh P, Hespanha J. Error amplification and disturbance propagation in vehicle strings with decentralized linear control. *44th IEEE Conference on Decision and Control*, IEEE, 2005; 4964 – 4969.
24. Jovanović MR, Bamieh B. On the ill-posedness of certain vehicular platoon control problems. *IEEE Trans. Automatic Control* September 2005; **50**(9):1307–1321.
25. Munz U, Papachristodoulou A, Allgower F. Robust Consensus Controller Design for Nonlinear Relative Degree Two Multi-Agent Systems With Communication Constraints. *Automatic Control, IEEE Transactions on* 2011; **56**(1):145–151.
26. Yadlapalli SK, Darbha S, Rajagopal KR. Information flow and its relation to stability of the motion of vehicles in a rigid formation. *IEEE Transactions on Automatic Control* August 2006; **51**(8).
27. Darbha S, Pagilla PR. Limitations of employing undirected information flow graphs for the maintenance of rigid formations for heterogeneous vehicles. *International journal of engineering science* 2010; **48**(11):1164–1178.
28. Veerman J. Stability of large flocks: an example July 2009. arXiv:1002.0768.
29. Bamieh B, Jovanovic M, Mitra P, Patterson S. Coherence in large-scale networks: Dimension dependent limitations of local feedback. *IEEE Transactions on Automatic Control, in press*, 2012; URL <http://arxiv.org/abs/1112.4011v1>.
30. Lin F, Fardad M, Jovanovic M. Optimal control of vehicular formations with nearest neighbor interactions. *IEEE Transactions on Automatic Control, in press*, 2012; URL <http://arxiv.org/abs/1112.4113v1>.
31. Stankovic S, Stanojevic M, Siljak D. Decentralized overlapping control of a platoon of vehicles. *Control Systems Technology, IEEE Transactions on* 2000; **8**(5):816–832.
32. Jovanovic M, Fowler J, Bamieh B, D'Andrea R. On avoiding saturation in the control of vehicular platoons. *Proc. American Control Conference*, vol. 3, 2004; 2257–2262.
33. Warnick S, Rodriguez A. Longitudinal control of a platoon of vehicles with multiple saturating nonlinearities. *American Control Conference*, vol. 1, IEEE, 1994; 403–407.
34. Khalil H. *Nonlinear Systems 3rd*. Prentice hall Englewood Cliffs, NJ, 2002.
35. Simon D. *Optimal state estimation: Kalman, H [infinity] and nonlinear approaches*. John Wiley and Sons, 2006.
36. Bamieh B, Dahleh M. Exact computation of traces and h2 norms for a class of infinite-dimensional problems. *Automatic Control, IEEE Transactions on* 2003; **48**(4):646–649.
37. Higham D. An algorithmic introduction to numerical simulation of stochastic differential equations. *SIAM review* 2001; **43**(3):525–546.
38. Hao H, Barooh P. Decentralized control of large vehicular formations: stability margin and sensitivity to external disturbances. *Arxiv preprint arXiv:1108.1409* 2011; URL <http://arxiv.org/abs/1108.1409>.
39. Hao H, Barooh P. Control of large 1D networks of double integrator agents: role of heterogeneity and asymmetry on stability margin. *IEEE Conference on Decision and Control*, 2010; 7395 – 7400. Expanded version: arXiv:1011.0791.
40. Hao H, Barooh P, Mehta PG. Stability margin scaling of distributed formation control as a function of network structure. *IEEE Transactions on Automatic Control* April 2011; **56**(4):923–929.
41. Hao H, Barooh P. On achieving size-independent stability margin of vehicular lattice formations with distributed control. *To appear in IEEE Transactions on Automatic Control*, October 2012; Expanded version: arXiv:1108.1844.
42. Hao H, Barooh P, Veerman J. Effect of network structure on the stability margin of large vehicle formation with distributed control. *Proceedings of the 49th IEEE conference on Decision and Control*, 2010.
43. Yueh W, Cheng S. Explicit eigenvalues and inverses of tridiagonal toeplitz matrices with four perturbed corners. *The Australian & New Zealand Industrial and Applied Mathematics (Anziam) Journal* 2008; **49**(3):361–388.
44. Haberman R. *Elementary applied partial differential equations: with Fourier series and boundary value problems*. Prentice-Hall, 2003.

## APPENDIX

*Proof of Theorem 1.* For the predecessor-following architecture with linear controller, it follows from straightforward algebra that the state matrix  $A$  can be written as

$$A = \begin{bmatrix} A_1 & & & & \\ A_2 & A_1 & & & \\ & & \ddots & \ddots & \\ & & & A_2 & A_1 \end{bmatrix}, \quad A_1 = \begin{bmatrix} 0 & 1 \\ -k_0 & -b_0 \end{bmatrix}, \quad A_2 = \begin{bmatrix} 0 & 0 \\ k_0 & b_0 \end{bmatrix}. \quad (24)$$

The state matrix  $A$  is a lower block triangular matrix, whose eigenvalues are determined by the block matrix  $A_1$  on the diagonal. The eigenvalues of  $A_1$  are  $\frac{-b_0 \pm \sqrt{b_0^2 - 4k_0}}{2}$ . Since there are  $N$  such block matrices on the diagonal of  $A$ , its eigenvalues have multiplicity  $N$ . Since the least stable eigenvalue is the one closest to the imaginary axis, it is given by  $\mu_1 = \frac{-b_0 + \sqrt{b_0^2 - 4k_0}}{2}$ , and this eigenvalue occurs with multiplicity  $N$ .

The result for the symmetric bidirectional architecture follows from Theorem 4 in [42] in a straightforward manner and is therefore omitted. ■

The proof of Theorem 2 will use the following proposition.

*Proposition 1*

Consider the second order autonomous system  $\dot{y}_1 = y_2, \dot{y}_2 = -f(y_1 - u_1) - g(y_2 - u_2)$ , where  $y_1, y_2, u_1, u_2 \in \mathbb{R}$  and the odd functions  $f, g : \mathbb{R} \rightarrow \mathbb{R}$  lie in the sectors  $f \in [\varepsilon_1, K_1], g \in [\varepsilon_2, K_2]$ , where  $0 < \varepsilon_1 \leq K_1 < \infty, 0 < \varepsilon_2 \leq K_2 < \infty$ . The origin of the unforced system (with  $u(t) = [u_1(t), u_2(t)]^T \equiv 0$ ) is globally exponentially stable (GES) and the system is input-to-state stable (ISS) with  $u$  as the input.  $\square$

*Proof of Proposition 1.* First, we consider the unforced system with state  $y = [y_1, y_2]^T$ ,

$$\dot{y}_1 = y_2, \quad \dot{y}_2 = -f(y_1) - g(y_2). \quad (25)$$

Consider the following Lyapunov function candidate:

$$V(y) = \frac{1}{2}y^T P y + \gamma \int_0^{y_1} f(z) dz, \quad (26)$$

where  $P = \begin{bmatrix} 1 & 1 \\ 1 & \gamma \end{bmatrix}$  and  $\gamma \geq \max\{1, \frac{1}{\varepsilon_2} + \frac{(1+K_2)^2}{\varepsilon_1 \varepsilon_2}\}$ , which ensures that  $P$  is positive definite.

From the Rayleigh Ritz Theorem [34], we have the following inequality  $\lambda_{\min}(P)\|y\|^2 \leq y^T P y \leq \lambda_{\max}(P)\|y\|^2$ , where  $\lambda_{\min}(P) > 0, \lambda_{\max}(P) > 0$  are the minimum and maximum eigenvalues of  $P$  respectively. This shows that  $V(y)$  is radially unbounded, and in addition satisfies the following

$$V(y) \leq \frac{\lambda_{\max}(P)}{2}\|y\|^2 + \frac{\gamma K_1}{2}y_1^2 \leq \frac{\lambda_{\max}(P) + \gamma K_1}{2}\|y\|^2, \quad (27)$$

where the second inequality follows from the fact that the function  $f(z)$  belongs to the sector  $[\varepsilon_1, K_1]$ . The derivative of  $V$  along the trajectory of (25) is given by

$$\begin{aligned} \dot{V} &= y^T P \dot{y} + \gamma f(y_1)y_2 = -y_1 f(y_1) - \gamma y_2 g(y_2) + y_2^2 + y_1 y_2 - y_1 g(y_2) \\ &\leq -\varepsilon_1 y_1^2 - (\gamma \varepsilon_2 - 1)y_2^2 + (1 + K_2)|y_1||y_2|, \\ &\leq -\frac{1}{2}(\varepsilon_1 y_1^2 + (\gamma \varepsilon_2 - 1)y_2^2) - \frac{1}{2}[\varepsilon_1 y_1^2 - 2(1 + K_2)|y_1||y_2| + (\gamma \varepsilon_2 - 1)y_2^2] \\ &\leq -\frac{1}{2}(\varepsilon_1 y_1^2 + (\gamma \varepsilon_2 - 1)y_2^2) \leq -\frac{1}{2} \min\{\varepsilon_1, (\gamma \varepsilon_2 - 1)\}\|y\|^2, \end{aligned} \quad (28)$$

where the second last inequality follows from  $\gamma \geq \max\{1, \frac{1}{\varepsilon_2} + \frac{(1+K_2)^2}{\varepsilon_1 \varepsilon_2}\}$ , upon a completion of squares. Since  $V$  is radially unbounded and satisfies (27), it follows from (28) that the origin  $y = 0$  of (25) is globally exponentially stable. Since the functions  $f, g$  are assumed to be smooth enough, the ISS property follows from the fact that a globally exponentially stable system with input  $u$  is ISS [34, Lemma 4.6].  $\blacksquare$

*Proof of Theorem 2.* We first consider the subsystem consisted of only the first agent. Its closed-loop dynamics can be written as below by using the fact  $\ddot{p}_0 = \dot{\dot{p}}_0 \equiv 0$ ,

$$\ddot{p}_1 = -f(\tilde{p}_1 - \tilde{p}_0) - g(\dot{\tilde{p}}_1 - \dot{\tilde{p}}_0) \Rightarrow \ddot{p}_1 = -f(\tilde{p}_1) - g(\dot{\tilde{p}}_1) \Rightarrow x^{(1)} = \mathbf{f}_1(x^{(1)}),$$

where  $x^{(1)} = [\tilde{p}_1, \dot{\tilde{p}}_1]^T$ . From Proposition 1, we have that the origin  $x^{(1)} = 0$  of the subsystem  $x^{(1)} = \mathbf{f}_1(x^{(1)})$  is GES. Next, we consider the subsystem consisted of the first two agents. Its closed-loop dynamics can be written as

$$\begin{cases} \ddot{p}_1 = -f(\tilde{p}_1) - g(\dot{\tilde{p}}_1), \\ \ddot{p}_2 = -f(\tilde{p}_2 - \tilde{p}_1) - g(\dot{\tilde{p}}_2 - \dot{\tilde{p}}_1), \end{cases} \Rightarrow x^{(1+2)} = \mathbf{f}_{1+2}(x^{(1+2)}),$$

where  $x^{(1+2)} = [\tilde{p}_1, \dot{\tilde{p}}_1, \tilde{p}_2, \dot{\tilde{p}}_2]^T$ . The above dynamics can be divided into two parts:

$$x^{(1+2)} = \mathbf{f}_{1+2}(x^{(1+2)}) \Rightarrow \begin{cases} x^{(1)} &= \mathbf{f}_1(x^{(1)}), \\ x^{(2)} &= \mathbf{f}_2(x^{(2)}, x^{(1)}), \end{cases} \quad (29)$$

where  $x^{(2)} = [\tilde{p}_2, \dot{\tilde{p}}_2]^T$ . The unforced system  $x^{(2)} = \mathbf{f}_2(x^{(2)}, 0)$  is given by

$$x^{(2)} = \mathbf{f}_1(x^{(2)}, 0) \Rightarrow \ddot{\tilde{p}}_2 = -f(\tilde{p}_2) - g(\dot{\tilde{p}}_2).$$

According to Proposition 1, the origin  $x^{(2)} = 0$  of the unforced system  $x^{(2)} = \mathbf{f}_2(x^{(2)}, 0)$  is GES and it's ISS with  $x^{(1)}$  as the input. We now invoke [34, Lemma 4.7], the origin of the cascade system  $x^{(1+2)} = \mathbf{f}_{1+2}(x^{(1+2)})$  given in (29) is globally asymptotically stable (GAS). We now prove the origin of the whole system is GAS by induction. Suppose the origin  $x^{(1+\dots+N-1)} = 0$  of the subsystem consisted of the first  $N-1$  agents  $x^{(1+\dots+N-1)} = \mathbf{f}_{1+\dots+N-1}(x^{(1+\dots+N-1)})$  is GAS, we consider the whole system, whose dynamics is given by

$$\dot{x} = \mathbf{f}(x) \Rightarrow x^{(1+\dots+N)} = \mathbf{f}_{1+\dots+N}(x^{(1+\dots+N)}).$$

The above dynamics can be divided into two parts:

$$x^{(1+\dots+N)} = \mathbf{f}_{1+\dots+N}(x^{(1+\dots+N)}), \Rightarrow \begin{cases} x^{(1+\dots+N-1)} &= \mathbf{f}_{1+\dots+N-1}(x^{(1+\dots+N-1)}), \\ x^{(N)} &= \mathbf{f}_N(x^{(N)}, x^{(1+\dots+N-1)}), \end{cases} \quad (30)$$

The unforced system  $x^{(N)} = \mathbf{f}_N(x^{(N)}, 0)$  is given by

$$x^{(N)} = \mathbf{f}_N(x^{(N)}, 0) \Rightarrow \ddot{\tilde{p}}_N = -f(\tilde{p}_N) - g(\dot{\tilde{p}}_N).$$

According to Proposition 1, the origin  $x^{(N)} = 0$  of the unforced system  $x^{(N)} = \mathbf{f}_N(x^{(N)}, 0)$  is GES and it's ISS with  $x^{(1+\dots+N-1)}$  as the input. Invoking [34, Lemma 4.7] again, we see that the origin  $x = x^{(1+\dots+N)} = 0$  of the whole system whose dynamics is given in (30) is globally asymptotically stable. This completes the proof by induction. ■

*Proof of Theorem 3.* For the 1-D network of double-integrator agents with symmetric bidirectional architecture, we consider the following Lyapunov function candidate, which is inspired by the one used in [25]:

$$V(x) = \sum_{i=1}^N \int_0^{\tilde{p}_i - \tilde{p}_{i-1}} f(z) dz + \frac{1}{2} \sum_{i=1}^N \dot{\tilde{p}}_i^2,$$

where  $x = [\tilde{p}_1, \dot{\tilde{p}}_1, \tilde{p}_2, \dot{\tilde{p}}_2, \dots, \tilde{p}_N, \dot{\tilde{p}}_N]$ . The derivative of  $V$  along the trajectory of (7) with  $w_i = 0$  is

$$\dot{V} = \sum_{i=1}^N f(\tilde{p}_i - \tilde{p}_{i-1})(\dot{\tilde{p}}_i - \dot{\tilde{p}}_{i-1}) + \sum_{i=1}^N \dot{\tilde{p}}_i \ddot{\tilde{p}}_i = - \sum_{i=1}^N (\dot{\tilde{p}}_i - \dot{\tilde{p}}_{i-1}) g(\dot{\tilde{p}}_i - \dot{\tilde{p}}_{i-1}) \leq 0,$$

If  $\dot{V} = 0$ , then we have  $\dot{\tilde{p}}_i = 0$  for all  $i$ , since  $g(z)$  satisfies  $zg(z) > 0, \forall z \neq 0$  and  $\dot{\tilde{p}}_0 = 0$  by definition. Asymptotic stability now follows from LaSalle's Invariance Principle. In addition, we have  $V(x) \rightarrow \infty$  as  $\|x\| \rightarrow \infty$ . Therefore, the Lyapunov function  $V$  is radially unbounded, and we get global asymptotic stability. ■

*Proof of Theorem 5.* Take Laplace transform of the coupled-ODE model (7) and assume zero initial conditions, the transfer function from the disturbance  $w = [w_1, \dots, w_N]^T$  to position error  $\tilde{p} = [\tilde{p}_1, \dots, \tilde{p}_N]^T$  is given by

$$G(s) = (s^2 I + (b_0 s + k_0) L)^{-1}, \quad (31)$$

where  $I$  is the  $N \times N$  identity matrix and  $L$  is given by

$$L = \begin{bmatrix} 2 & -1 & & & \\ -1 & 2 & -1 & & \\ & \ddots & \ddots & \ddots & \\ & & -1 & 2 & -1 \\ & & & -1 & 1 \end{bmatrix}. \quad (32)$$

Following Theorem 3.1 of [43], the eigenvalues of  $L$  and its corresponding orthonormal eigenvectors are given by

$$\lambda_\ell = 2 - 2 \cos\left(\frac{(2\ell - 1)\pi}{2N + 1}\right) = 4 \sin^2\left(\frac{(2\ell - 1)\pi}{2(2N + 1)}\right), \quad (33)$$

$$v_\ell = \frac{2}{\sqrt{2N + 1}} \left[ \sin\left(\frac{(2\ell - 1)\pi}{2N + 1}\right), \dots, \sin\left(\frac{(2\ell - 1)N\pi}{2N + 1}\right) \right]^T. \quad (34)$$

(1) *For the case of first-to-last amplification*, the transfer function  $G_{FTL}$  from disturbance  $w_1$  on the first agent to the position error of the last agent  $\tilde{p}_N$  is  $G_{FTL} = \phi_N^T G(s) \phi_1$ , where  $\phi_i$  is the  $i$ -th canonical basis vector of  $\mathbb{R}^N$  whose  $i$ -th entry is 1 and the rest are all 0's. Therefore,

$$\begin{aligned} G_{FTL}(s) &= \phi_N^T M (s^2 I + (b_0 s + k_0) \Lambda)^{-1} M^T \phi_1 \\ &= \phi_N^T M \begin{bmatrix} \frac{1}{s^2 + \lambda_1 b_0 s + \lambda_1 k_0} & & \\ & \ddots & \\ & & \frac{1}{s^2 + \lambda_N b_0 s + \lambda_N k_0} \end{bmatrix} M^T \phi_1 \\ &= \frac{4}{2N + 1} \sum_{\ell=1}^N \left( \sin \frac{(2\ell - 1)N\pi}{2N + 1} \sin \frac{(2\ell - 1)\pi}{2N + 1} G_\ell(s) \right), \end{aligned} \quad (35)$$

where  $M = [v_1, v_2, \dots, v_N]$ ,  $\Lambda = \text{diag}(\lambda_1, \lambda_2, \dots, \lambda_N)$  such that  $L = M \Lambda M^T$  and

$$G_\ell(s) := \frac{1}{s^2 + \lambda_\ell b_0 s + \lambda_\ell k_0}. \quad (36)$$

It can be shown using straightforward calculus that for each eigenvalue  $\lambda_\ell$ , the maximum amplitude and its peak frequency of  $G_\ell(s)$  are

$$A_\ell := \max_{\omega} |G_\ell(j\omega)| = \begin{cases} \frac{2}{\lambda_\ell^{3/2} b_0 \sqrt{4k_0 - \lambda_\ell b_0^2}}, & \text{if } \lambda_\ell \leq 2k_0/b_0^2, \\ \frac{1}{\lambda_\ell k_0}, & \text{otherwise.} \end{cases} \quad (37)$$

$$\omega_\ell := \arg \max |G_\ell(j\omega)| = \begin{cases} \frac{\sqrt{4\lambda_\ell k_0 - 2\lambda_\ell^2 b_0^2}}{2}, & \text{if } \lambda_\ell \leq 2k_0/b_0^2, \\ 0, & \text{otherwise.} \end{cases} \quad (38)$$

From (33),  $\lambda_1 < \lambda_2 < \dots < \lambda_N$ , which can be used to show by straightforward algebra that  $A_1 > A_2 > \dots > A_N$ . For future use, we have from  $\frac{2}{\pi} \theta \leq \sin \theta \leq \theta, \forall \theta \in [0, \frac{\pi}{2}]$  that

$$\frac{4(2\ell - 1)^2}{(2N + 1)^2} \leq \lambda_\ell \leq \frac{(2\ell - 1)^2 \pi^2}{(2N + 1)^2}. \quad (39)$$

We first express  $G_{FTL}(s)$  in (35) as

$$G_{FTL}(s) = T(s) + Z(s), \quad (40)$$

where

$$T(s) = \frac{4}{2N+1} \sin \frac{N\pi}{2N+1} \sin \frac{\pi}{2N+1} G_1(s), \quad (41)$$

$$Z(s) = \frac{4}{2N+1} \sum_{\ell=2}^N \left( \sin \frac{(2\ell-1)N\pi}{2N+1} \sin \frac{(2\ell-1)\pi}{2N+1} G_\ell(s) \right). \quad (42)$$

Now,

$$\begin{aligned} \sup_{\omega} |G_{FTL}(j\omega)| &\leq \sup_{\omega} |T(j\omega)| + \sup_{\omega} |Z(j\omega)| = |T(j\omega_1)| + \sup_{\omega} |Z(j\omega)|, \\ \sup_{\omega} |G_{FTL}(j\omega)| &\geq |T(j\omega_1) + Z(j\omega_1)| \geq |T(j\omega_1)| - |Z(j\omega_1)|, \end{aligned}$$

where  $\omega_1$  is given in (38). Combining the above two inequalities, we obtain

$$|T(j\omega_1)| - |Z(j\omega_1)| \leq \sup_{\omega} |G(j\omega)| \leq |T(j\omega_1)| + \sup_{\omega} |Z(j\omega)|. \quad (43)$$

We now derive an upper bound for  $\sup_{\omega} |Z(j\omega)|$ . Using triangle inequality, it follows from (42) satisfies

$$\begin{aligned} \sup_{\omega} |Z(j\omega)| &\leq \frac{4}{2N+1} \sum_{\ell=2}^N \left( \sin \frac{(2\ell-1)N\pi}{2N+1} \sin \frac{(2\ell-1)\pi}{2N+1} \sup_{\omega} |G_\ell(j\omega)| \right) \\ &\leq \frac{4}{2N+1} \sum_{\ell=2}^N \left( \sin \frac{(2\ell-1)\pi}{2N+1} A_\ell \right) \leq \frac{4}{2N+1} \sum_{\ell=2}^N \frac{(2\ell-1)\pi}{2N+1} A_\ell, \end{aligned} \quad (44)$$

where the last inequality follows from the fact that  $\sin \theta \leq \theta$  for  $\theta \in [0, \pi/2]$  and  $\frac{(2\ell-1)\pi}{2N+1} \in [0, \pi/2]$  for  $2 \leq \ell \leq N$ . From Eq. (37), we notice that depending on whether  $\lambda_\ell \leq 2k_0/b_0^2$  or not, the expressions of  $A_\ell$ 's are different. First we have

$$\lambda_\ell \leq 2k_0/b_0^2 \quad \Rightarrow \quad \frac{1}{4k_0 - \lambda_\ell b_0^2} \leq \frac{1}{2k_0}, \quad \text{and} \quad \lambda_\ell > 2k_0/b_0^2 \quad \Rightarrow \quad \frac{1}{\lambda_\ell} < \frac{b_0^2}{2k_0}. \quad (45)$$

Let  $N_c$  be the index so that  $\ell \leq N_c \Rightarrow \lambda_\ell \leq 2k_0/b_0^2$  and  $\ell > N_c \Rightarrow \lambda_\ell > 2k_0/b_0^2$ . The inequality in (44) can be written as

$$\begin{aligned} \sup_{\omega} |Z(j\omega)| &\leq \frac{4}{2N+1} \left( \sum_{\ell=2}^{N_c} \frac{(2\ell-1)\pi}{2N+1} \frac{2}{\lambda_\ell^{3/2} b_0 \sqrt{4k_0 - \lambda_\ell b_0^2}} + \sum_{\ell=N_c}^N \frac{(2\ell-1)\pi}{2N+1} \frac{1}{\lambda_\ell k_0} \right) \\ &\leq \frac{4}{(2N+1)^2} \sum_{\ell=2}^N \left( \frac{(2\ell-1)\pi}{\sqrt{2k_0} b_0} \frac{2}{\lambda_\ell^{3/2}} + (2\ell-1)\pi \frac{b_0^2}{2k_0^2} \right). \end{aligned} \quad (46)$$

From (39), we have  $\frac{1}{\lambda_\ell^{3/2}} \leq \frac{(2N+1)^3}{8(2\ell-1)^3}$ . The inequality (46) becomes

$$\begin{aligned} \sup_{\omega} |Z(j\omega)| &\leq \frac{\pi(2N+1)}{\sqrt{2k_0} b_0} \sum_{\ell=2}^N \frac{1}{(2\ell-1)^2} + \frac{2b_0^2\pi}{k_0^2(2N+1)^2} \sum_{\ell=2}^N (2\ell-1) \\ &\leq \frac{\pi(2N+1)}{4\sqrt{2k_0} b_0} \sum_{\ell=2}^{\infty} \frac{1}{(\ell-1)^2} + \frac{2b_0^2\pi}{k_0^2(2N+1)^2} \sum_{\ell=2}^N (2\ell-1) \\ &\leq \frac{\pi(2N+1)}{4\sqrt{2k_0} b_0} \left( \frac{\pi^2}{6} - 1 \right) + \frac{2b_0^2\pi}{k_0^2(2N+1)^2} (N^2 - 1), \end{aligned} \quad (47)$$

where the last inequality follows from  $\sum_{\ell=1}^{\infty} \frac{1}{\ell^2} = \frac{\pi^2}{6}$  and  $\sum_{\ell=1}^N (2\ell - 1) = N^2$ . This proves an upper bound for  $\sup_{\omega} |Z(j\omega)|$ .

We now obtain an upper bound for  $|T(j\omega_1)|$

$$\begin{aligned} |T(j\omega_1)| &= \frac{4}{2N+1} \sin \frac{N\pi}{2N+1} \sin \frac{\pi}{2N+1} A_1 \leq \frac{4}{2N+1} \frac{\pi}{2N+1} A_1 \\ &\leq \frac{4}{2N+1} \frac{\pi}{2N+1} \frac{2}{\lambda_1^{3/2} b_0 \sqrt{4k_0 - \lambda_1 b_0^2}} + \frac{4}{2N+1} \frac{\pi}{2N+1} \frac{1}{\lambda_1 k_0} \\ &\leq \frac{4\pi}{(2N+1)^2} \frac{(2N+1)^3}{4b_0 \sqrt{2k_0}} + \frac{4\pi}{(2N+1)^2} \frac{b_0^2}{2k_0^2} \leq \frac{\pi(2N+1)}{b_0 \sqrt{2k_0}} + \frac{2b_0^2 \pi}{k_0^2 (2N+1)^2}, \end{aligned} \quad (48)$$

Substituting inequalities (47) and (48) into (43), we get a upper bound for  $\sup_{\omega} |G_{FTL}(j\omega)|$

$$\sup_{\omega} |G_{FTL}(j\omega)| \leq \left( \frac{\pi^3 + 18\pi}{12b_0 \sqrt{2k_0}} \right) N + c_1, \quad (49)$$

where  $c_1$  is a constant independent of  $N$ .

To prove the lower bound for  $|T(j\omega_1)|$ , we first use the fact that  $\frac{2}{\pi}\theta \leq \sin \theta, \forall \theta \in [0, \frac{\pi}{2}]$ ,

$$\begin{aligned} |T(j\omega_1)| &= \frac{4}{2N+1} \sin \frac{N\pi}{2N+1} \sin \frac{\pi}{2N+1} A_1 \\ &\geq \frac{4}{2N+1} \frac{2}{\pi} \frac{N\pi}{2N+1} \frac{2}{\pi} \frac{\pi}{2N+1} A_1 \geq \frac{16N}{(2N+1)^3} A_1. \end{aligned} \quad (50)$$

For any fixed  $k_0, b_0$ , when  $N$  is large, we have  $\lambda_1 < 2k_0/b_0^2$ , which implies

$$A_1 = \frac{2}{\lambda_1^{3/2} b_0 \sqrt{4k_0 - \lambda_1 b_0^2}} \geq \frac{1}{\lambda_1^{3/2} b_0 \sqrt{k_0}} \geq \frac{1}{b_0 \sqrt{k_0}} \frac{(2N+1)^3}{\pi^3}, \quad (51)$$

where the last inequality is obtained from (39). The inequality (50) now becomes

$$|T(j\omega_1)| \geq \frac{16N}{\pi^3 b_0 \sqrt{k_0}}. \quad (52)$$

In addition, we have

$$|Z(j\omega_1)| \leq \frac{4}{2N+1} \sum_{\ell=2}^N \left( \frac{(2\ell-1)\pi}{2N+1} |G_{\ell}(j\omega_1)| \right) \leq \frac{4}{2N+1} \sum_{\ell=2}^N \left( \frac{(2\ell-1)\pi}{2N+1} \frac{1}{\lambda_{\ell} k_0 \sqrt{(1-\lambda_1/\lambda_2)^2}} \right).$$

From (39), we obtain that  $\frac{1}{\lambda_{\ell}} \leq \frac{(2N+1)^2}{4(2\ell-1)^2}$ ,  $\frac{\lambda_1}{\lambda_2} \leq \frac{\pi^2}{36}$ . Thus the above inequality can be simplified to

$$|Z(j\omega_1)| \leq 2c_2 \sum_{\ell=2}^N \left( \frac{(2\ell-1)}{(2N+1)^2} \frac{(2N+1)^2}{4(2\ell-1)^2} \right) \leq 2c_2 \sum_{\ell=2}^N \left( \frac{1}{(2\ell-1)} \right) \leq c_2 \sum_{\ell=1}^{N-1} \frac{1}{\ell},$$

where  $c_2 = \frac{\pi}{2k_0 \sqrt{(1-\pi^2/36)^2}}$  is a constant independent of  $N$ . Moreover,  $\sum_{\ell=1}^{N-1} \frac{1}{\ell} = 1 + \sum_{\ell=2}^{N-1} \frac{1}{\ell} \leq 1 + \int_1^{N-1} \frac{1}{s} ds$ , we have  $\sum_{\ell=1}^{N-1} \frac{1}{\ell} \leq 1 + \ln(N-1)$ . Thus, we have

$$|Z(j\omega_1)| \leq c_2 \ln(N-1) + c_2. \quad (53)$$

Substituting inequalities (53) and (52) into (43), we get a lower bound for  $\sup_{\omega} |G_{FTL}(j\omega)|$

$$\sup_{\omega} |G_{FTL}(j\omega)| \geq \frac{16N}{\pi^3 b_0 \sqrt{k_0}} - c_2 \ln(N-1) - c_2. \quad (54)$$



In addition, when  $N$  is large, the constants  $c_1, c_2$  and the  $O(\ln(N-1))$  term are dominated by the  $O(N)$  term, therefore we ignore them in (49) and (54) respectively, we obtain

$$\left(\frac{16}{\pi^3 b_0 \sqrt{k_0}}\right)N \leq A_{FTL}^{linear} \leq \left(\frac{\pi^3 + 18\pi}{12b_0 \sqrt{2k_0}}\right)N.$$

(2) For the case of all-to-all amplification, the transfer function from the disturbance  $w = [w_1, \dots, w_n]$  on all the agents to their position tracking errors  $\tilde{p} = [\tilde{p}_1, \dots, \tilde{p}_N]$  are given by

$$\begin{aligned} G_{ATA}(s) &= G(s) = (s^2 I + (b_0 s + k_0)L)^{-1} = M(s^2 I + (b_0 s + k_0)\Lambda)^{-1} M^T \\ &= M \begin{bmatrix} G_1(s) & & \\ & \ddots & \\ & & G_N(s) \end{bmatrix} M^T, \end{aligned} \quad (55)$$

where  $G_\ell(s)$  is given in (36) and  $M$  is the orthonormal matrix given as before. The  $H_\infty$  norm of  $G_{ATA}(s)$  (i.e.  $A_{ATA}^{linear}$ ) is now given by

$$\begin{aligned} \|G_{ATA}\|_{H_\infty} &= \sup_{\omega} \|G_{ATA}(j\omega)\|_2 = \sup_{\omega} \sqrt{\lambda_{\max}(G_{ATA}^*(j\omega)G_{ATA}(j\omega))} \\ &= \sup_{\omega} \max_{\ell} \frac{1}{\sqrt{(-\omega^2 + \lambda_\ell k_0)^2 + b_0^2 \omega^2 \lambda_\ell^2}} = \max_{\omega} \max_{\ell} \|G_\ell(j\omega)\| = \max_{\ell} A_\ell = A_1, \end{aligned}$$

where  $A_1$  is given in (37). Again for large  $N$ , we obtain from (51),

$$A_1 \geq \frac{1}{b_0 \sqrt{k_0}} \frac{(2N+1)^3}{\pi^3}. \quad (56)$$

In addition, using  $\lambda_1 < 2k_0/b_0^2$  and  $\frac{1}{\lambda_\ell^{3/2}} \leq \frac{(2N+1)^3}{8}$ , we have

$$A_1 = \frac{2}{\lambda_1^{3/2} b_0 \sqrt{4k_0 - \lambda_1 b_0^2}} \leq \frac{2}{\lambda_1^{3/2} b_0 \sqrt{2k_0}} \leq \frac{(2N+1)^3}{4b_0 \sqrt{2k_0}}. \quad (57)$$

Combining (56) and (57), we obtain

$$\left(\frac{1}{b_0 \sqrt{k_0} \pi^3}\right)(2N+1)^3 \leq A_{ATA}^{linear} \leq \left(\frac{1}{4b_0 \sqrt{2k_0}}\right)(2N+1)^3, \quad \forall N.$$

To get the asymptotic formula, when  $N$  is large, we use the approximation  $\lambda_1 \approx \frac{\pi^2}{4N^2}$ . Therefore,  $\lambda_1 < 2k_0/b_0^2$  is true for large enough  $N$  irrespective of the values of  $k_0$  and  $b_0$ . Substituting  $\lambda_1 \approx \frac{\pi^2}{4N^2}$  into (37) and (38), we obtain that  $A_1 \approx \frac{8N^3}{\sqrt{k_0} b_0 \pi^3}$ ,  $\omega_p = \omega_1 \approx \frac{\sqrt{k_0} \pi}{2N}$ . Since  $A_{ATA}^{linear} = A_1$ , this concludes the proof. ■

*Proof of Corollary 1.* We first rewrite the coupled-ODE model (7) with linear controller as

$$\ddot{\tilde{p}} + b_0 L \dot{\tilde{p}} + k_0 L \tilde{p} = v_1 \sin(\omega_1 t), \quad (58)$$

where  $L$  is given in (32) and  $v_1$  is the eigenvector of  $L$  corresponding to the smallest eigenvalue  $\lambda_1$  given in (34). By the method of eigenfunction expansion [44], we can write  $\tilde{p}(t) = \sum_{\ell=1}^N v_\ell h_\ell(t)$ , where  $v_\ell$ 's are the eigenvectors of  $L$  given in (34). Substituting it into Eq. (58), we obtain

$$\sum_{\ell=1}^N (v_\ell \ddot{h}_\ell(t) + b_0 L v_\ell \dot{h}_\ell(t) + k_0 L v_\ell h_\ell(t)) = v_1 \sin(\omega_1 t).$$

Due to superposition property of linear system, the above equation can be split into  $N$  ordinary differential equations by using  $Lv_\ell = \lambda_\ell v_\ell$ ,

$$\begin{aligned}\ddot{h}_1(t) + b_0\lambda_1\dot{h}_1(t) + k_0\lambda_1h_1(t) &= \sin(\omega_1t), \\ \ddot{h}_\ell(t) + b_0\lambda_\ell\dot{h}_\ell(t) + k_0\lambda_\ell h_\ell(t) &= 0, \quad \ell \in \{2, \dots, N\}.\end{aligned}$$

Following straightforward algebra, the steady-state response of each  $h_\ell(t)$  is given by

$$h_1(t) = A_1 \sin(\omega_1t + \psi_1), \quad h_\ell(t) = 0, \quad \ell \in \{2, \dots, N\},$$

where  $A_1$  is given in (37). Thus the steady state response of  $\tilde{p}$  is given by  $\tilde{p} = v_1 A_1 \sin(\omega_1t + \psi_1)$ , which yields  $\frac{\|\tilde{p}\|_{\mathcal{L}_2}}{\|w\|_{\mathcal{L}_2}} = A_1$ . Recall from Theorem 5 that  $A_{ATA}^{linear} = A_1$ , we complete the proof. ■

A ‘‘proof’’ of the conjecture is as follows. First notice that

$$A_{FTL}^{linear} = \sup_{\omega} |G_{FTL}(j\omega)| \leq \sup_{\omega} |T(j\omega)| + \sup_{\omega} |Z(j\omega)| = |T(j\omega_1)| + \sup_{\omega} |Z(j\omega)|$$

When  $N$  is large, the smallest eigenvalue  $\lambda_1 \approx \frac{\pi^2}{4N^2}$  and  $\sin \frac{N\pi}{2N+1} \approx 1$ . The expression  $|T(j\omega_1)|$  are then approximately given by

$$|T(j\omega_1)| \approx \frac{4}{2N+1} \frac{\pi}{2N+1} A_1 \approx \frac{4}{2N+1} \frac{\pi}{2N+1} \frac{(2N+1)^3}{b_0\sqrt{k_0}\pi^3} \approx \frac{8N}{\sqrt{k_0}b_0\pi^2}. \quad (59)$$

Under the assumption  $N$  is large, the  $O(N)$  term in the upper bound of  $\sup_{\omega} |Z(j\omega)|$  which is given in (47) dominates the  $O(1)$  term. Moreover, this  $O(N)$  term is still smaller than  $|T(j\omega_1)|$  given in (59). Notice that this upper bound is obtained by letting each term in  $|Z(j\omega)|$  containing  $G_\ell(j\omega)$  ( $\ell \in \{1, 2, \dots, N\}$ ) to achieve their maximum. In fact, the maximum of  $|G_{FTL}(j\omega)|$  can be only achieved at a single frequency. We thus conjecture that this frequency should be equal to  $\omega_1$ , the peak frequency corresponding to the principal model  $\lambda_1$ . This idea is similar to that a wave equation’s resonance is achieved at the peak frequency correspond to its principle mode [44] and its  $H_\infty$  norm is determined by the peak response of the principle mode. Now, the  $H_\infty$  norm of  $G_{FTL}(s)$  is given by  $\|G_{FTL}(j\omega)\| = |G(j\omega_1)|$ . Thus from (40), we have

$$|T(j\omega_1)| - |Z(j\omega_1)| \leq \sup_{\omega} |G(j\omega)| \leq |T(j\omega_1)| + |Z(j\omega_1)|$$

When  $N \gg 1$ , the lower and upper bound will be dominated by the term  $|T(j\omega_1)|$ , since  $|Z(j\omega_1)|$  is  $O(\ln(N-1))$  but  $|T(j\omega_1)|$  is  $O(N)$ . Thus the  $H_\infty$  norm of  $G_{FTL}(s)$  is determined by  $|T(j\omega_1)|$ . From (59), we have the first-to-last amplification  $A_{FTL}^{linear} \approx |T(j\omega_1)| = \frac{8N}{\sqrt{k_0}b_0\pi^2}$ .